# PART Ⅲ VAN YEN AREA

# PART III VAN YEN AREA

## CHAPTER 1. REGIONAL GEOLOGICAL SURVEY

### 1.1. Survey Methods

Conventional field methods were used for geological survey. Topographic maps at a scale of 1:10,000 enlarged from the 1:50,000 published maps were used in the field and route mapping was carried out at this scale. Photogeological interpretation using aerial photographs was supplementally conducted for mapping in some areas without field reconnaissance. Localities in the field were sometimes confirmed by means of GPS (global positioning system). Results of the geological survey were compiled on geological map at a scale of 1:50,000.

### 1.2. Geologic Setting

This survey area belongs to the "West Bacbo" tectonic province. This province is a mobile belt lying between the South China Plate to the north and the Indochina Plate to the south, and is called the "Da River Mobile Belt". This belt is a submerged zone which was produced by the separation of the above two plates during the Indosinian stages (from the Late Carboniferous to Late Triassic). The igneous activities occurred along the submerged zone and their chemical compositions range from ultramafic to felsic.

This area is underlain chiefly by the Proterozoic metamorphic basement and the overlying Paleozoic and Mesozoic sedimentary (partly metamorphic) and pyroclastic rocks. The Proterozoic rocks consist mainly of gneisses and occur in the northeastern and southeastern parts of this area. The Paleozoic strata occur in the whole of the survey area, and consist of Cambrian to Permian marine sediments represented mainly by limestone, sandstone, and mudstone. The Mesozoic is composed of Triassic pyroclastic and sedimentary rocks. Although large intrusive masses have not been found in this area, granitic rocks and small bodies of gabbroic rocks occur mainly in the Proterozoic area. They extend in the same direction as the structural trend of the Proterozoic rocks. Numerous ultramafic bodies are also recognized in the central part of the survey area.

### 1.3. Stratigraphy

The basement of this area comprises the Proterozoic metamorphic rocks represented mainly by gneisses. Unconformably overlying the basement are metamorphic and sedimentary rocks of Cambrian to Permian time, pyroclastic and sedimentary rocks of Triassic (Early and Late) time, and unconsolidated Quaternary sediments. Thus the whole survey area is divided into 10 geologic units. Figure Ⅲ-1-1 shows the schematic columnar sections, and the geologic map and sections are given in Figures Ⅲ-1-2 and Ⅲ-1-3, respectively. Since the objective of the field work of this phase is not to pursue the detailed lithology of the geologic units, they are divided into "Group", "Systems", and "Series". Moreover the complicated symbols given to the units of the published geologic maps were simplified for the compilation of this phase as shown in Figure Ⅲ-1-2. The description of the intrusive rocks will be discussed in section 1.4.

(1) Proterozoic Group (PR)

This Group occurs in the northeastern and southeastern parts of this area and comprises the basement of the area. The Group generally trends in the NW-SE direction with 2 km and 5 km width in the northeast and more than 10 km in the southeast. The PR area of the southeastern part extends outside the survey area eastward. The Group is mainly made up of grey course-grained biotite gneiss with partly intercalated strata of amphibole gneiss, green schist, pelitic schist, psammitic schist, and quartzite. The gneisses show migmatic lithofacies in some parts and mylonitic facies are also found near faults.

The biotite gneiss represents conspicuous gneissosities and cataclastic texture is partly observed under microscope. The gneiss consists of abundant plagioclase and subordinate amounts of quartz and biotite as major constituent minerals.

The Group is estimated to be 2,000 m thick in this area.

(2) Upper Cambrian to Lower Ordovician Series ($Є_3O_1$)

This Series occurs as three blocks separately in the northeastern part (one block) and the southeastern part (2 blocks) of the survey area. All blocks trend in the NW-SE direction with 2 to 4 km width. These blocks are present in the vicinity of the PR Group and unconformably overlies the Group in most parts.

The major part of the Series in the northeast is made up of dark grey phyllitic mudstone and a few strata of the lower part is altered to pelitic schist. The northern block of the southeastern part consists mostly of light purple to dark purple coarse-grained sandstone with some amounts of

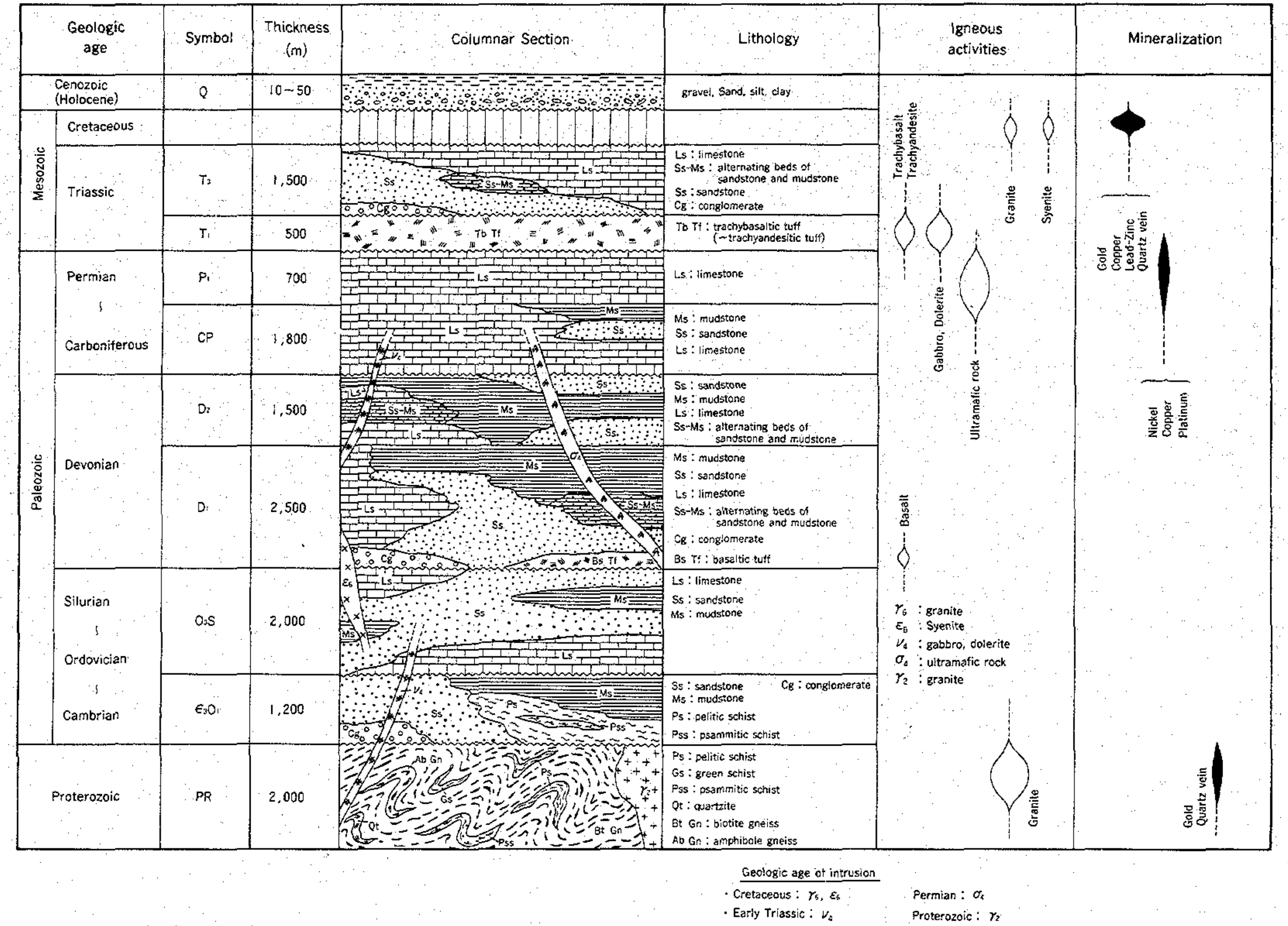


**Fig.Ⅲ-1-1 Schematic Columnar Sections of the Van Yen Area**

conglomerates of the same rock type. Abundant potash feldspar are contained in the matrix of the sandstone, and the conglomerate is composed of quartzite and green rock pebbles of 1 to 4 cm in diameter. The southern block, on the other hand, comprises alternating beds of pelitic schist, grey siliceous fine-grained sandstone, and grey psammitic schist.

The thickness of this Series is estimated to be 1,200 m in the survey area.

(3) Upper Ordovician Series to Silurian System ($O_3S$)

This geologic unit is present only in the southern part of the survey area (on both banks of the Da River). The unit roughly trends in the NW-SE direction with 4 to 7 km width. The major part of the unit is made up of grey hard compact siliceous sandstone, and its grain size varies from fine to coarse. Some horizons of the lower and upper parts are dominated by grey siliceous limestone beds, and black phyllitic mudstone is intercalated in the middle part.

This unit is estimated to be 2,000 m thick in the survey area.

(4) Lower Devonian Series ($D_1$)

This Series occurs separately in the northern, central, and southern parts of the survey area. The Series extends in the WNW-ESE to E-W and NW-SE to NNW-SSE directions in the north and south, respectively. The extending direction in the central part is not clear. The widths are 4 to 5 km, 1 to 2 km, and 2 to 3 km (2 belts) in the northern, central, and southern parts, respectively. The major parts of the northern and central parts are made up of grey to light grey fine- to medium-grained sandstone. The middle to upper part of these blocks becomes dominant in black to dark grey phyllitic mudstone and contains some alternating beds of sandstone and mudstone. The southern block is dominated by grey limestone whose bedding is developed with intervals of about a meter. Moreover, brownish grey basalt and its (partly andesitic) lapilli tuff and tuff breccia are intercalated in small areas of this Series located in the east-central and southern parts.

The estimated thickness of the Series in the area is 2,500 m.

(5) Middle Devonian Series ($D_2$)

This Series occupies very wide parts of the survey area such as the northern, central, and southern (the mountains in the right bank of the Da

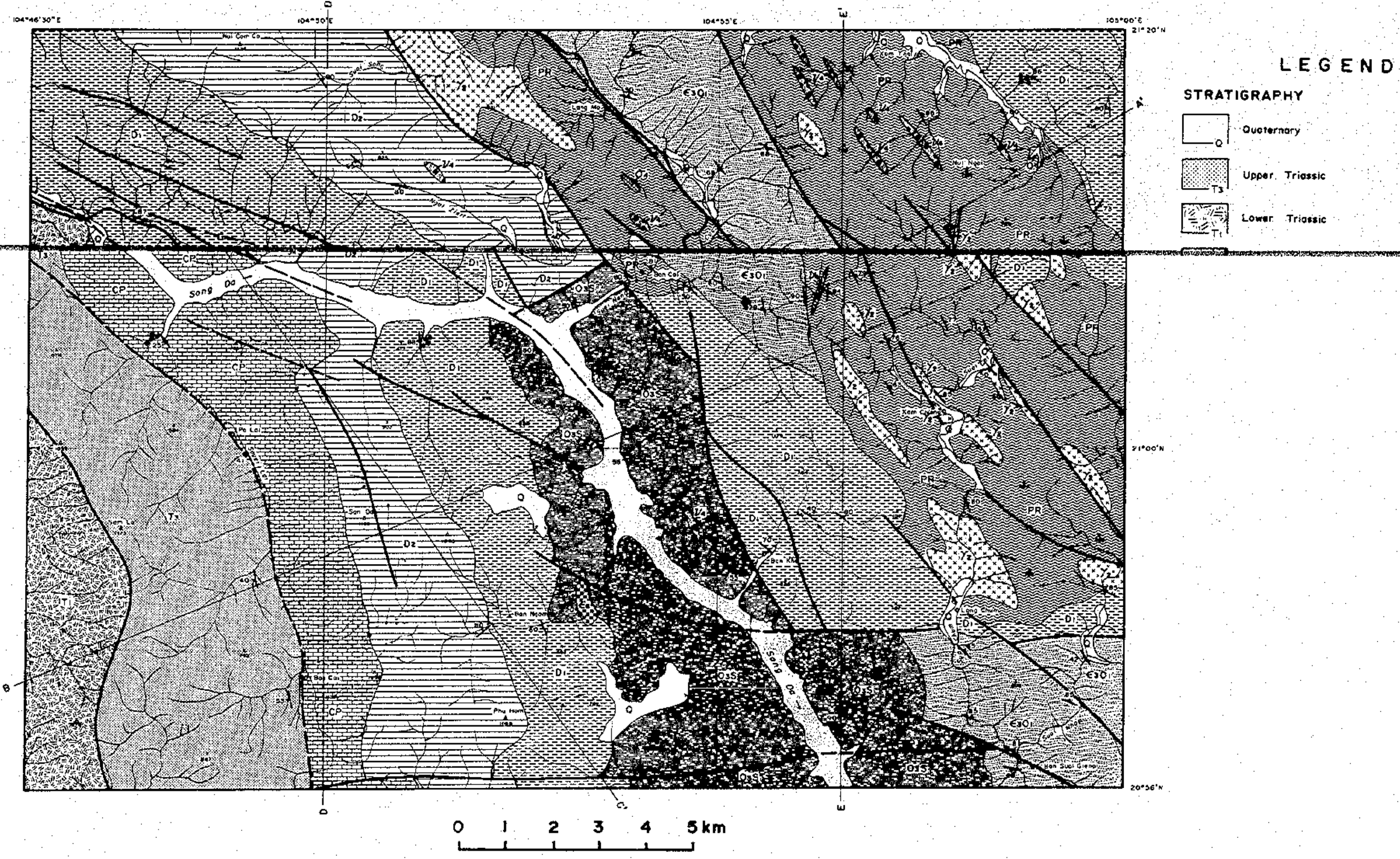


Fig.Ⅲ-1-2 Geologic Map of the Van Yen Area

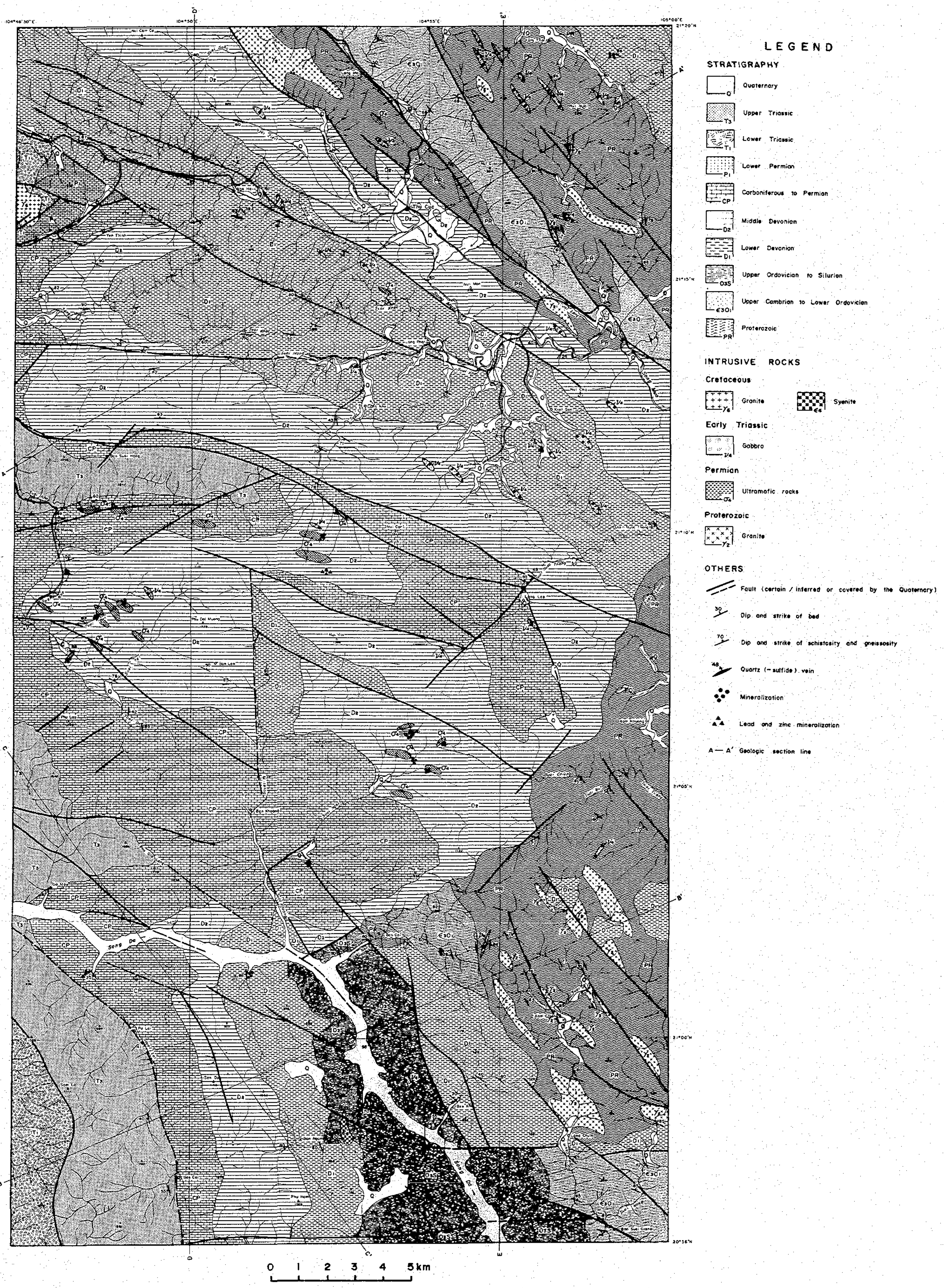


Fig.Ⅲ-1-2 Geologic Map of the Van Yen Area

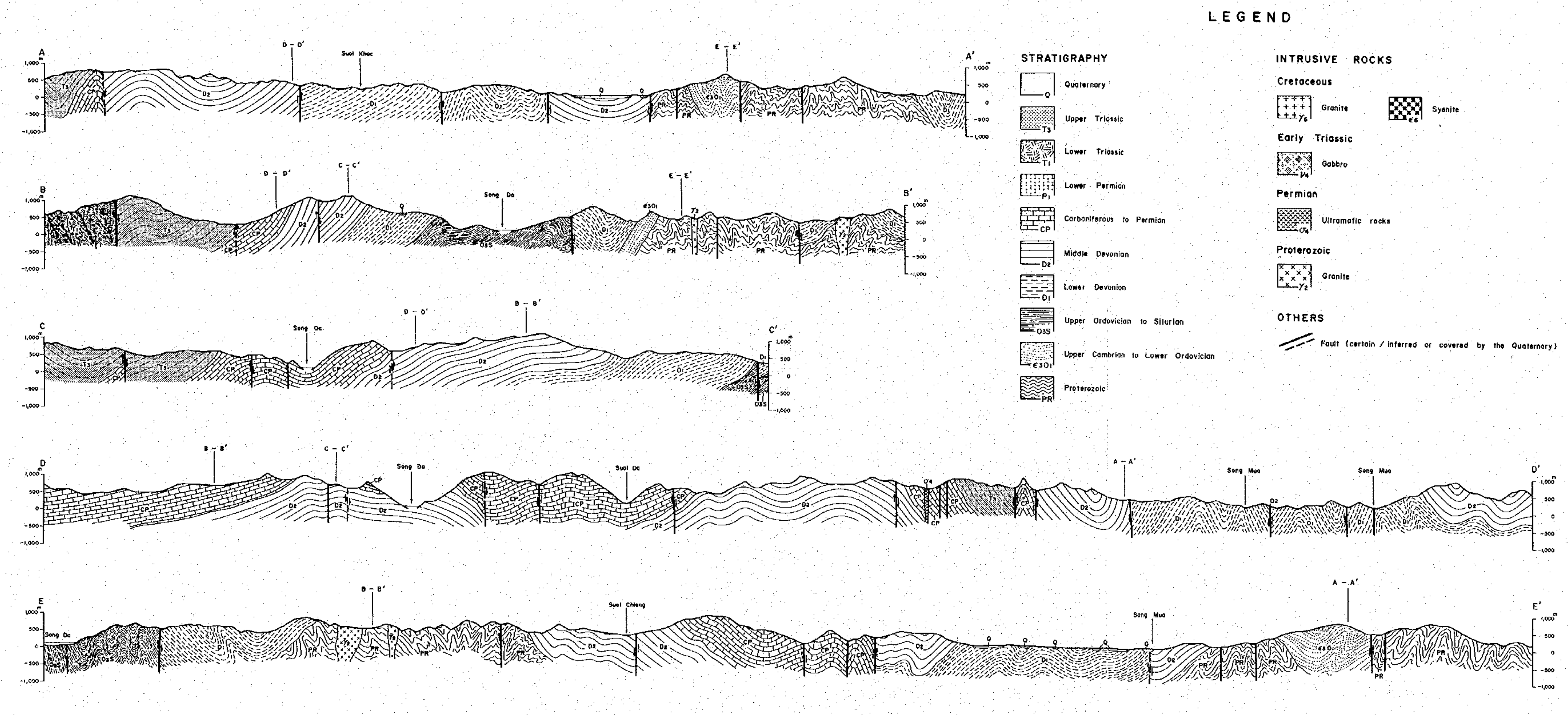


Fig.Ⅲ-1-3 Geologic Sections of the Van Yen Area

River) parts, and unconformably overlies all underlying geologic unit except the Lower Devonian ($D_1$). This Series forms very steep folded mountains together with the $D_1$ Series and Carboniferous to Permian System (CP; mentioned later). The extending directions differ from part by part, and the Series has NW-SE, E-W, and N-S trends in the northern, central, and southern parts, respectively. The widths are 2 to 3 km, 2 to 5 km, and 2 to 3 km in the northern, central, and southern parts, respectively.

The major part of the Series is made up of black to dark grey phyllitic mudstone. Grey massive limestone is present in the northern basal part and it overlies the PR Group. The lower and upper horizons of the central parts are dominated by grey to light grey fine-grained sandstone and the middle horizon consists of alternating beds of fine-grained sandstone and mudstone with intervals several centimeters apart. The Series in the southern part is composed of limestone and sandstone.

This Series is estimated to be 1,500 m thick in the survey area.

(6) Carboniferous to Permian System (CP)

This System occurs in northwestern, central, and southern parts of the area. The System unconformably overlies the $D_1$ Series and occupies the zone around the Series. The major parts of the System extend generally in the E-W to WNW-ESE direction. On the contrary, it has the N-S trend in the right bank of the Da River in the south. Although the average width is 2 km, it attains 6 km in a wider part with a fault. The System is composed generally of grey to dark grey massive fine-grained limestone and tower karsts are formed in many places. Fire-grained sandstone and sandy mudstone are intercalated in this Series of the southern part.

The estimated thickness of the Series in the area is 1,800 m.

(7) Lower Permian Series ($P_1$)

This Series is present as a small area in the northwestern edge of the survey area and is in fault contact with the CP System. The Series is located in the northern flank of the anticlinorium formed by the $D_1$-$D_2$-CP Series and System, and trends in the ENE-WSW direction with 1 to 2 km width. The Series consists as a whole of dark grey massive limestone in the area.

The estimated thickness of the Series in the area is 700 m.

(8) Lower Triassic Series ($T_1$)

This Series occurs as small areas in the northwestern and southwestern edges of the survey area. In the northwestern edge it is present on the west of the $P_1$ Series. Both blocks extend continuously from the survey area of Phase I. The major part of the Series is made up of dark green trachybasaltic (to trachyandesitic) fine tuff whose schistosity is well developed.

The Series is estimated to be 500 m thick in this survey area.

(9) Upper Triassic Series ($T_3$)

This Series occurs separately in the central and southern parts of the area and is in unconformable or fault contact with the underlying CP System and $T_1$ Series. This Series is present around the CP System in the folded mountains formed by the $D_1$-$D_2$-CP Series and System. The lower part of the Series generally is dominated by dark grey fine- to very fine-grained sandstone and the upper part by dark grey limestone. Besides the middle part of the Series consists partly of alternating beds of dark grey very fine-grained sandstone and black mudstone with constant intervals 10 cm apart. Some conglomerate beds are found in the basal part.

The Series is estimated to be 1,500 m thick in the survey area.

(10) Quaternary System (Q)

The Quaternary System in this area is composed of fan sediments, recent fluviatile sediments and others which correspond to the Holocene alluvium. The sediments consist of gravel, sand, silt, and clay. These sediments are present widely in the intra-montane basin where Thu Cuc is located and many streams flow in from the surrounding steep mountains. The sediments occur also along the lower reaches of the Bua River and its tributaries as well as along the Suoi Chum. In other parts, for instance, along the tributaries of the Da, upper reaches of the Bua Rivers, and the Suoi Khoang, the sediments hardly occur due to extremely intense downward erosion since those tributaries are all rapids with short extension.

### 1.4. Intrusive Rocks

Abundant intrusive bodies formed by igneous activities during Proterozoic and Permian to Cretaceous times occur in this survey area. The lithology of these rocks is divided into several types such as granitic, ultramafic to mafic, alkali felsic rocks. Generally the rock bodies are of small dimensions. No intrusive rock was found in the $D_1$, $D_2$, CP, and $T_3$ areas in the southwestern part of the survey area, where all geologic units are sedimentary rocks. Their lithology will be described below in the order of intrusion (GSV, 1991).

(1) Proterozoic granitic rocks ($\gamma_2$)

The granitic rocks intruded into the PR Group in the northeastern and southeastern parts of the area. Six and 11 bodies are observed in the northeastern and southeastern parts, respectively. The bodies range in width from 200 to 500 m with the maximum observed length of 4 km and more.

Generally the rocks are light pink to light pinkish grey medium-grained biotite granites and major trend of intrusion is NW-SE. Weak gneissosities are partly observed and some rocks represent tonalitic lithofacies. Microscopic studies reveal that crystals of potash feldspar, plagioclase, quarts, and small amounts of biotite form holocrystalline equigranular texture.

The whole rock analysis of the representative rock samples has revealed the following chemical composition.

| Sample No. | $SiO_2$ | $TiO_2$ | $Al_2O_3$ | $Fe_2O_3$ | FeO | MnO | MgO | CaO | $Na_2O$ | $K_2O$ | $P_2O_5$ | LOI |
|---|---|---|---|---|---|---|---|---|---|---|---|---|
| VGR 62 | 71.39 | 0.31 | 14.01 | 1.13 | 1.22 | 0.01 | 0.64 | 0.23 | 2.31 | 7.01 | 0.08 | 1.25 |
| VGR 66 | 77.23 | 0.09 | 11.50 | 1.03 | 0.42 | 0.01 | 0.23 | 0.11 | 2.31 | 5.20 | 0.01 | 1.33 |

Unit: percent

(2) Permian ultramafic rocks ($\sigma_4$)

The ultramafic rocks intruded in the form of sheet and dike into mostly sedimentary rocks of the $D_2$ Series and CP System in the central part of the area. Twenty two bodies are observed in the whole of the area. Also more rock bodies are believed to be exposed, because floats of these rocks were frequently recognized in the streams that flow into the Suoi Nho and Suoi Can. The bodies range in width from 20 to 200 m with the maximum observed length of 1.3 km.

Generally the rocks are black to dark green compact peridotites and major trend of intrusion is E-W to WNW-ESE. Microscopic studies reveal that crystals of olivine, clinopyroxene, and plagioclase form granoblastic texture and the olivine is often replaced by serpentine.

The list below shows the results of whole rock analysis of the representative rock samples.

| Sample No. | $SiO_2$ | $TiO_2$ | $Al_2O_3$ | $Fe_2O_3$ | FeO | MnO | MgO | CaO | $Na_2O$ | $K_2O$ | $P_2O_5$ | LOI |
|---|---|---|---|---|---|---|---|---|---|---|---|---|
| VMR 54 | 39.49 | 0.59 | 4.53 | 5.78 | 5.87 | 0.17 | 27.80 | 3.93 | 0.06 | 0.11 | 0.06 | 9.51 |
| VAR 56 | 40.51 | 0.72 | 6.20 | 2.40 | 9.17 | 0.20 | 25.20 | 4.67 | 0.06 | 0.06 | 0.06 | 8.26 |
| VBR 54 | 41.88 | 0.71 | 6.28 | 4.13 | 6.84 | 0.17 | 24.89 | 6.73 | 0.35 | 0.15 | 0.08 | 5.49 |

Unit: percent

(3) Early Triassic gabbro and dolerite ($\nu_4$)

These rocks were recognized at 29 localities in this area. Most of them are sporadically scattered in the whole survey area except for the southwestern Paleozoic and Mesozoic areas. Generally the rock bodies are exposed in small dimensions and intrude as dikes. The trend of intrusion is NW-SE to WNW-ESE with two exceptions of NE-SW, and it coincides with the strike of intruded rocks. The rock bodies are several meters wide with a maximum of 300 m, and range in length from several hundreds meters to 1.0 km. The density of distribution is high in the northeastern part of the PR Group area, where nine bodies are present.

These rocks are divided lithologically into two types: dark green gabbro (to metagabbro) and dolerite (to metadolerite). In general the former is more abundant than the latter. Microscopic studies reveal that both types show ophitic texture and consist mainly of clinopyroxene and plagioclase, with occasional accessory hornblende and actinolite.

The whole rock analysis of a metagabbroic rock sample has revealed the following chemical composition.

| Sample No. | $SiO_2$ | $TiO_2$ | $Al_2O_3$ | $Fe_2O_3$ | FeO | MnO | MgO | CaO | $Na_2O$ | $K_2O$ | $P_2O_5$ | LOI |
|---|---|---|---|---|---|---|---|---|---|---|---|---|
| VMR 57 | 49.24 | 1.99 | 12.27 | 4.56 | 12.97 | 0.26 | 4.86 | 7.52 | 1.84 | 2.02 | 0.76 | 1.21 |

Unit: percent

(4) Cretaceous granite ($\gamma_6$)

Only one granite body was recognized within the area of the $T_1$ Series in the northwestern edge of this area. The body extends outside toward the survey area of Phase I, thus the dimension is 1 to 2 km in diameter.

The rock is white medium- to coarse-grained holocrystalline equigranular biotite granite.

(5) Cretaceous syenite ($\varepsilon_6$)

Only one syenite body intruded into limestone of the units $O_3S$ and $D_1$ in the southern part of this area. The rock is 100 to 150 m wide as a small dike and it seems that the trend of intrusion is N-S.

This rock is generally pink and porphyritic. Microscopic studies reveal that the texture is holocrystalline porphyritic and both groundmass and phenocrysts consist of a large amount of potash feldspars.

The list below shows the results of whole rock analysis of the representative rock sample.

| Sample No. | $SiO_2$ | $TiO_2$ | $Al_2O_3$ | $Fe_2O_3$ | FeO | MnO | MgO | CaO | $Na_2O$ | $K_2O$ | $P_2O_5$ | LOI |
|---|---|---|---|---|---|---|---|---|---|---|---|---|
| VSR 52 | 73.06 | 0.25 | 13.49 | 0.69 | 0.73 | <0.01 | 0.67 | 0.31 | 2.13 | 7.44 | 0.07 | 0.90 |

Unit: percent

### 1.5. Geologic Structure

(1) Folds

There is a considerable disparity of the structural trends of rocks between the southwestern part and other parts within all over the area. The southwestern part has structural trends of N-S to NNW-SSE, where the CP System and $T_3$ Series form folds with 4 km wavelength. The other parts of the survey area are characterized by the structural trend of NW-SE to WNW-ESE to E-W.

Regionally traceable key beds do not exist in the sedimentary units of the survey area. For instance, a specific tuff bed within the alternating beds of sandstone and mudstone, or a well continuous mudstone bed within pyroclastic rocks can be a good key bed. Apart from this, the formation of rifts during the Indosinian stages and subsequent collision of plates took place in and around this area. Thus, it is said that the area was subjected to intense and complex tectonic movements. As a result of the movements, the beds have enormously steep dip in the most parts of this area. Therefore, the overall and detailed features of foldings are very difficult to discern. Nevertheless, gneissosities, schistosities, and bedding planes are well developed in most metamorphic rocks, sandstone, and mudstone. On the basis of the above structural elements including minor folds observed in the field, the macroscopic folds can be interpreted as shown in Figure Ⅲ-1-3. The available geologic map and sections were referred for the parts with poor field data.

The characteristics of folds in each geologic unit are summarized as follows (excluding the $P_1$ and $T_1$ Series).

1) Proterozoic Group (PR)

Gneisses and schists of this Group generally have a constant strike of NW-SE direction and steep dips of more than 60°. The metamorphic rocks show extremely complicated structure affected by several diastrophic disturbances. The Group consists of a series of NW-SE trending anticline and syncline with about 500 m wavelength, and those folds are believed to form large anticlinoriums both in the northeastern and southeastern parts of the area.

2) Upper Cambrian to Lower Ordovician Series ($Є_3O_1$)

The strata of the Series generally strike NW-SE and steeply dip NE or SW both in northeastern and southeastern parts of the area. This Series consists of a series of NW-SE trending folds with 0.5 to 1 km wavelength, and those folds as a whole are considered to form anticlinoriums in both parts.

3) Upper Ordovician Series to Silurian System ($O_3S$)

The strata generally strike NW-SE to NNW-SSE and have steep dips. The northern part of this unit consists of a series of NNW-SSE trending folds with about 3 km wavelength, and those folds form a large anticlinorium. On the contrary, geologic structure is not clear in the southern part of this unit. Nevertheless the unit of this part is inferred to form a synclinorium by a series of folds with about 1 km wavelength.

4) Lower Devonian Series ($D_1$)

This Series generally strikes WNW-ESE to E-W in the northern part, but the strike changes to NW-SE in the southeastern part of the area. Most of the strata steeply dip more than 50°. A large anticlinorium is formed by a series of WNW-ESE to E-W trending folds with about 1.5 km wavelength in the northern part, and it plunges to the west. In the southeastern part of the area the Series consists of NW-SE trending folds with about 2 km wavelength, but it is not clear whether those folds form an anticlinorium or a synclinorium because this Series is confined to small areas.

5) Middle Devonian Series ($D_2$)

This Series generally strikes WNW-ESE in the northern edge, and E-W in the northern to central part of the survey area. The strata steeply dip more than 50°. The Series forms a syncline with about 3 km wavelength in the northern edge. On the contrary, in the northern to central part of the area the Series consists of a series of folds with 1.0 to 2.5 km wavelength, and those folds form two large anticlinoriums together with the underlying $D_1$ Series. Both of them plunge to the west.

6) Carboniferous to Permian System, Upper Triassic Series (CP, $T_3$)

These geologic units occur surrounding the $D_2$ Series, and have folds similar to the Series in the northern to central part of the survey area. That is, the major part of these units generally strikes E-W, and a series of E-W trending folds form two large anticlinoriums together with the $D_2$ Series. Most of strata have steep beds, but moderate to gentle beds are also often observed. The wavelength of individual fold in the units CP and $T_3$ is estimated to be 3 to 4 km.

(2) Faults

There are four systems of faults in this area. They are NW-SE, WNW-ESE to E-W, N-S, and NE-SW systems. These faults occur in a complex pattern and the order of formation on those fault systems is not clear. With regard to the structural trend of the strata, there are two kinds of faults. That is, one is concordant with the general trend of rocks of each geologic unit, and the other is oblique to the trend. Most of the faults in this survey area are in concordance with the general trend of rocks. The lengths of the faults vary considerably, ranging from 3 to more than 20 km. Relatively large vertical displacement has been calculated to be more than 2,000 m.

## 1.6. Mineralization

No widespread mineralization zone has not been found in this regional survey area as described in Chapter 2 of Part Ⅱ. Three zones are recognized with high density of localities where gold grains were microscopically confirmed by the past exploratory work (panning). However, with respect to the lead-zinc and platinum-copper-nickel mineralization, only several mineral showings have been discovered. And no mineral deposit is presently under operation in this area. The following characteristics regarding mineralization were elucidated during the course of this survey. Figure Ⅲ-1-4 shows the distribution of investigated mineral showings.

### 1.6.1. Gold mineralization

Native gold grains from the panned concentrate samples were confirmed microscopically at nine localities by this survey as mentioned later in the section 2.2. Although the origin of these grains is supposed to be hydrothermal gold-bearing quartz veins, the essential characteristics of primary deposits still remain unknown through this field survey. Quartz veins, stockwork of quartz, and floats of quartz vein were found at eight localities in this area, and samples were collected for chemical analysis. Table Ⅲ-1-1 shows the characteristics of those quartz veins investigated by the present survey. The maximum width of the quartz veins is 1 m, and it attains to 2 m in the case of the stockwork. It appears that no specified tendency is recognized in regard to host rock, dip and strike of the veins. The gold contents of the samples are all less than 2 ppb, and this indicates that the gold mineralization is very weak in these veins.

1.6.2. Lead-zinc mineralization

This mineralization is characterized by the hydrothermal vein-type deposits which are hosted by Middle Devonian and Carboniferous to Permian limestone. Three mineral showings of this type have been found in this area and the Suoi Can mineral showing is the representative one. The Suoi Can mineral showing was examined in the course of this survey because this showing has larger dimensions than the others and there was topographical difficulty to access the others.

【Suoi Can mineral showing】

This mineral showing is located on the north-facing slope of the uppermost reaches of the Can Stream (altitude: 1,080 m), a tributary of the Khac Stream in the central part of the area (see Figure Ⅲ-1-4). It takes about two hours on foot from the last stop of a car-road to this showing. A trench trending in the N30°E has been made by the Geological Mapping Division of GSV. The trench is 2 to 3 m wide, 1.5 m deep, and 8 m long (Figure Ⅲ-1-5). The ore body is hosted by Middle Devonian grey massive limestone, and consists of vein-type ore along a fracture that has a N30°W strike and a vertical dip. The vein-type ore zone comprises the mixture of crushed white limestone powder and aggregate of brecciated ore. Only galena is observed not only in the field but under microscope, and no other metallic minerals are recognized. Gangue minerals are calcite, dolomite, and quartz. The vein-type ore body is exposed with 30 cm width and 70 cm length. The ore body does not continue southeastward and pinches out there. The host rock limestone has been crushed into powder with 1 to 2 cm width on both sides along the ore body.

The assay results of samples collected from the ore body are as follows.

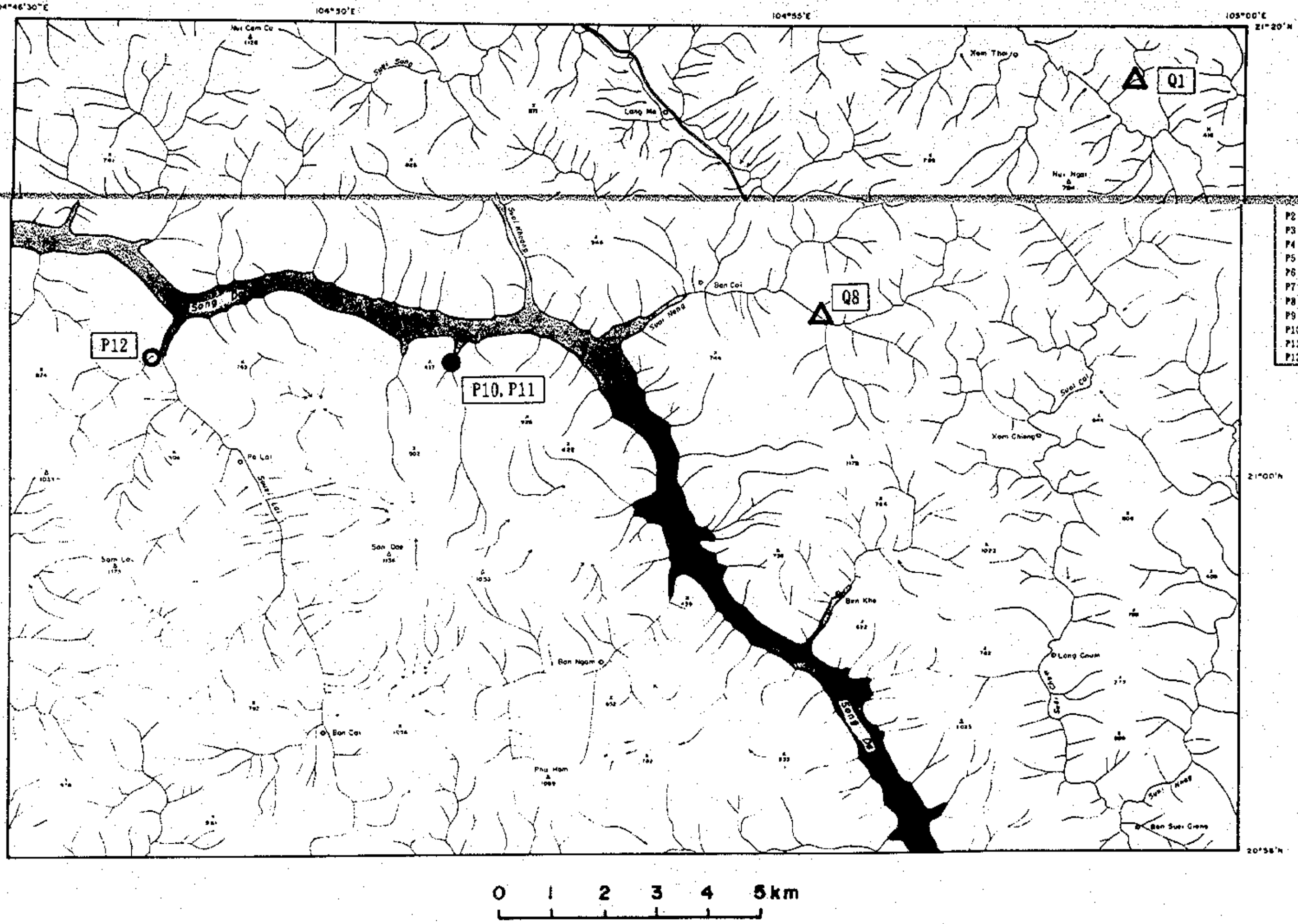


LEGEND

Mineralization

Outcrop

| | | | | | | | | | | | |
|---|---|---|---|---|---|---|---|---|---|---|---|
| P2 | VAN57 | - | <2 | <2 | <0.001 | 0.026 | 0.201 | 0.019 | 0.039 | 0.174 | <5 |
| P3 | VNN52 | 0.3 | <2 | <2 | <0.001 | 0.002 | 0.005 | 0.001 | 0.030 | 0.003 | <5 |
| P4 | VNN53 | 3.0 | <2 | <2 | <0.001 | 0.004 | 0.019 | 0.003 | 0.030 | 0.009 | <5 |
| P5 | VAN58 | 0.2 | <2 | <2 | 0.012 | <0.001 | <0.001 | <0.001 | <0.001 | 0.030 | <5 |
| P6 | VAN59 | 0.2 | <2 | <2 | 0.007 | <0.001 | <0.001 | <0.001 | <0.001 | 0.026 | <5 |
| P7 | VAN60 | - | <2 | <2 | <0.001 | 0.002 | 0.018 | 0.003 | 0.004 | 0.056 | <5 |
| P8 | VAN61 | - | <2 | <2 | 0.001 | <0.001 | 0.034 | 0.006 | 0.044 | 0.109 | <5 |
| P9 | VAN64 | - | <2 | <2 | <0.001 | <0.001 | <0.001 | 0.002 | 0.021 | 0.003 | <5 |
| P10 | VAN66 | - | <2 | <2 | <0.001 | 0.002 | 0.001 | 0.002 | 0.015 | 0.029 | <5 |
| P11 | VAN67 | 0.2 | <2 | <2 | 0.002 | 0.003 | 0.014 | 0.002 | 0.006 | 0.025 | <5 |
| P12 | VAN68 | - | <2 | <2 | <0.001 | <0.001 | 0.004 | <0.001 | 0.017 | 0.153 | <5 |

Fig.Ⅲ-1-4 Distribution Map of the Mineral Showings in the Van Yen Area

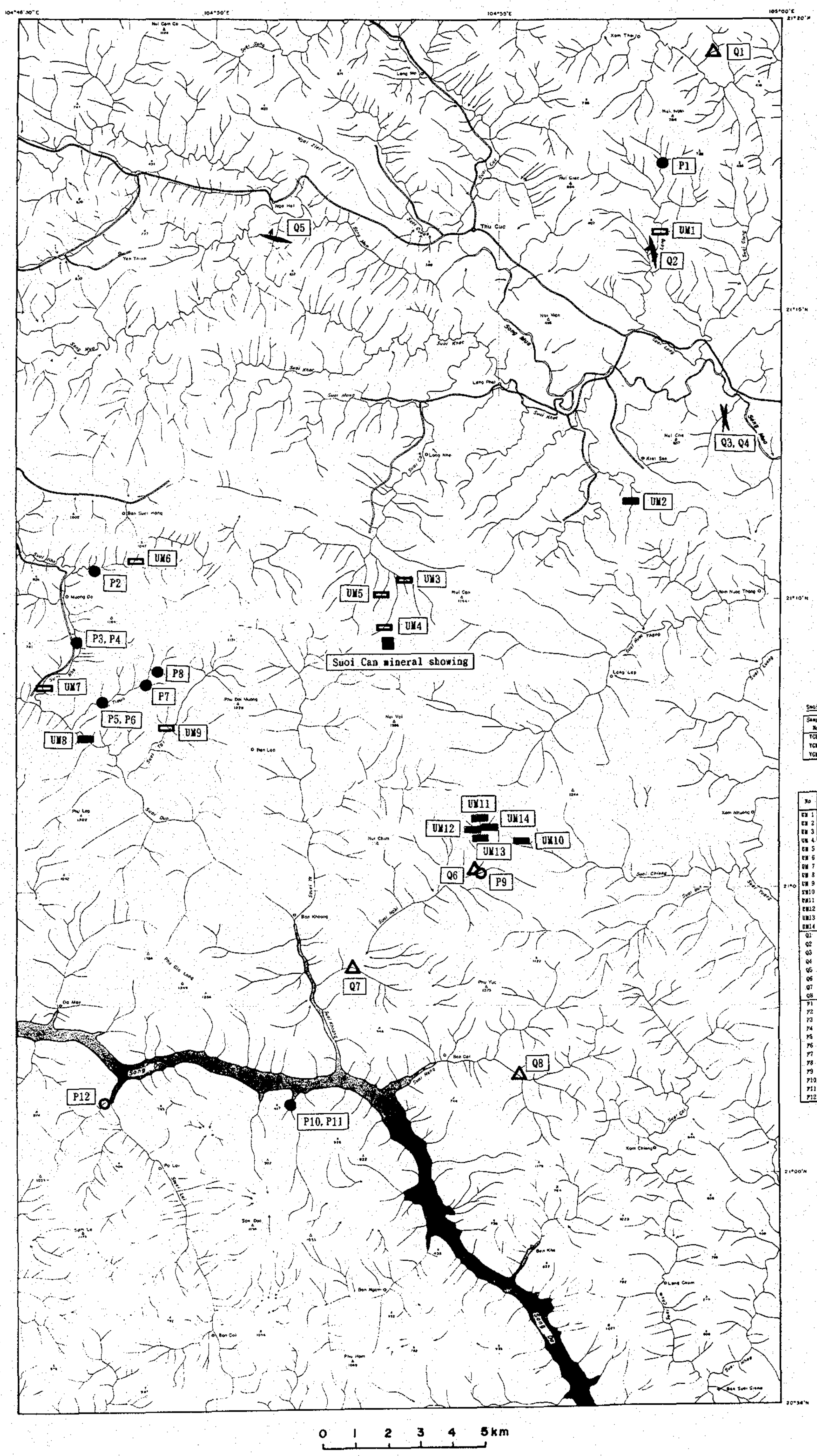


L E G E N D

Mineralization

Outcrop

- Quartz vein
- Pyritization zone
- Lead mineralization
- Ultramafic rock

Float

- Quartz vein
- Pyrite dissemination
- Ultramafic rock

Location of sample for chemical analysis
Q 1:Quartz vein
P 1:Pyrite dissemination
UM1:Ultramafic rock

Suoi Can mineral showing

| Sample No. | Wd m | Au ppb | Ag ppm | Cu % | Pb % | Zn % | Ni % | Cr % | Mn % | Pt ppb |
|---|---|---|---|---|---|---|---|---|---|---|
| YCN82 | 1.0 | <2 | <2 | <0.001 | 0.713 | 0.002 | 0.001 | 0.002 | 0.007 | <5 |
| YCN87 | 0.6 | <2 | 53 | <0.001 | 8.861 | 0.012 | <0.001 | 0.016 | 0.007 | <5 |
| YCN83 | 1.0 | <2 | <2 | <0.001 | 0.019 | 0.010 | <0.001 | <0.001 | 0.012 | <5 |

| No | Sample No. | wd m | Au ppb | Ag ppm | Cu % | Pb % | Zn % | Ni % | Cr % | Mn % | Pt ppb |
|---|---|---|---|---|---|---|---|---|---|---|---|
| UM 1 | VCN60 | - | <2 | <2 | 0.007 | 0.002 | 0.047 | 0.010 | 0.012 | 0.161 | <5 |
| UM 2 | VCN51 | - | <2 | <2 | 0.005 | <0.001 | 0.018 | 0.034 | 0.112 | 0.143 | 5 |
| UM 3 | VCN52 | - | <2 | <2 | 0.010 | <0.001 | 0.024 | 0.081 | 0.102 | 0.118 | 10 |
| UM 4 | VCN93 | - | <2 | <2 | 0.005 | 0.197 | 0.425 | 0.114 | 0.169 | 0.103 | 15 |
| UM 5 | VCN81 | - | <2 | <2 | 0.011 | <0.001 | 0.026 | 0.133 | 0.107 | 0.108 | 10 |
| UM 6 | VAN56 | - | <2 | <2 | 0.005 | <0.001 | 0.052 | 0.111 | 0.108 | 0.136 | 15 |
| UM 7 | VBN54 | - | <2 | <2 | 0.008 | <0.001 | 0.036 | 0.118 | 0.159 | 0.122 | 10 |
| UM 8 | VNN54 | - | <2 | <2 | 0.004 | 0.002 | 0.024 | 0.130 | 0.152 | 0.116 | 15 |
| UM 9 | VBN55 | - | <2 | <2 | 0.005 | <0.001 | 0.031 | 0.111 | 0.133 | 0.115 | 10 |
| UM10 | M1-1 | - | <2 | <2 | 0.009 | 0.003 | 0.019 | 0.096 | 0.183 | 0.135 | 15 |
| UM11 | M2-2 | - | <2 | <2 | 0.017 | 0.002 | 0.005 | 0.052 | 0.245 | 0.088 | 40 |
| UM12 | M3-1 | - | <2 | <2 | 0.011 | 0.008 | 0.005 | 0.033 | 0.245 | 0.072 | 35 |
| UM13 | M4 | - | <2 | <2 | 0.055 | 0.002 | 0.005 | 0.044 | 0.231 | 0.072 | 35 |
| UM14 | M5 | - | <2 | <2 | 0.015 | 0.002 | 0.006 | 0.036 | 0.258 | 0.075 | 20 |
| Q1 | VCN64 | - | <2 | <2 | 0.002 | <0.001 | <0.001 | 0.002 | 0.031 | 0.023 | <5 |
| Q2 | VCN59 | - | <2 | <2 | 0.012 | <0.001 | <0.001 | 0.003 | 0.025 | 0.006 | <5 |
| Q3 | VCN56 | 2.0 | <2 | <2 | 0.002 | 0.002 | <0.001 | 0.002 | 0.032 | 0.008 | <5 |
| Q4 | VCN57 | 2.0 | <2 | <2 | <0.001 | <0.001 | 0.001 | 0.002 | 0.057 | 0.010 | <5 |
| Q5 | VBN53 | 0.5 | <2 | <2 | <0.001 | <0.001 | <0.001 | 0.003 | 0.026 | 0.005 | <5 |
| Q6 | VAN62 | - | <2 | <2 | <0.001 | <0.001 | <0.001 | 0.002 | 0.017 | 0.007 | <5 |
| Q7 | VAN65 | - | <2 | <2 | <0.001 | <0.001 | <0.001 | 0.002 | 0.017 | 0.010 | <5 |
| Q8 | VNN55 | - | <2 | <2 | 0.456 | 0.017 | <0.001 | 0.003 | 0.038 | 0.053 | <5 |
| P1 | VCN63 | - | <2 | <2 | <0.001 | 0.008 | 0.048 | 0.014 | 0.015 | 0.409 | <5 |
| P2 | VAN57 | - | <2 | <2 | <0.001 | 0.026 | 0.201 | 0.019 | 0.039 | 0.178 | <5 |
| P3 | VNN52 | 0.3 | <2 | <2 | <0.001 | 0.002 | 0.005 | 0.001 | 0.030 | 0.003 | <5 |
| P4 | VNN53 | 3.0 | <2 | <2 | <0.001 | 0.004 | 0.019 | 0.003 | 0.030 | 0.009 | <5 |
| P5 | VAN58 | 0.2 | <2 | <2 | 0.012 | <0.001 | <0.001 | <0.001 | <0.001 | 0.030 | <5 |
| P6 | VAN59 | 0.2 | <2 | <2 | 0.007 | <0.001 | <0.001 | <0.001 | <0.001 | 0.026 | <5 |
| P7 | VAN60 | - | <2 | <2 | <0.001 | 0.002 | 0.018 | 0.003 | 0.004 | 0.056 | <5 |
| P8 | VAN61 | - | <2 | <2 | 0.001 | <0.001 | 0.034 | 0.006 | 0.044 | 0.109 | <5 |
| P9 | VAN64 | - | <2 | <2 | <0.001 | <0.001 | <0.001 | 0.002 | 0.021 | 0.003 | <5 |
| P10 | VAN66 | - | <2 | <2 | <0.001 | 0.002 | 0.001 | 0.002 | 0.015 | 0.029 | <5 |
| P11 | VAN67 | 0.2 | <2 | <2 | 0.002 | 0.008 | 0.014 | 0.002 | 0.006 | 0.025 | <5 |
| P12 | VAN68 | - | <2 | <2 | <0.001 | <0.001 | 0.004 | <0.001 | 0.017 | 0.153 | <5 |

Fig.Ⅲ-1-4 Distribution Map of the Mineral Showings in the Van Yen Area

Table Ⅲ-1-1 Characteristics of Quartz Veins in the Van Yen Area

| No. | Sample locality | Occurrence | Host rock | Mineral assemblage | Sample No. | Dimensions & trend (m) | Ore grade | | | | | | | | |
|---|---|---|---|---|---|---|---|---|---|---|---|---|---|---|---|
| | | | | | | | Au ppb | Ag ppm | Cu % | Pb % | Zn % | Ni % | Cr % | Mn % | Pt ppb |
| Q1 | Eastern Xom Thoi | Floats (Stockwork) | Phyllitic Shale | — | VGM 64 | — | < 2 | < 2 | 0.002 | < 0.001 | < 0.001 | 0.002 | 0.031 | 0.023 | < 5 |
| Q2 | Middle reaches of the Suoi Lang | Vein | Biotite Gneiss | — | VGM 59 | 1×5×10 N6W ,48W | < 2 | < 2 | 0.012 | < 0.001 | < 0.001 | 0.001 | 0.025 | 0.006 | < 5 |
| Q3 | Song Mua | Stockwork | Sandstone | Qtz,Py dissemination | VGM 56 | 2.0 wd | < 2 | < 2 | 0.002 | 0.002 | < 0.001 | 0.002 | 0.032 | 0.008 | < 5 |
| Q4 | Song Mua | Stockwork | Sandstone | Qtz,Py dissemination | VGM 57 | 2.0 wd | < 2 | < 2 | < 0.001 | < 0.001 | 0.001 | 0.002 | 0.057 | 0.010 | < 5 |
| Q5 | Nga Hai | Vein | Mudstone | Qtz | VBM 53 | N80W ,83N Wd=0.5 | < 2 | < 2 | < 0.001 | < 0.001 | <0.001 | 0.001 | 0.026 | 0.005 | < 5 |
| Q6 | Upper reaches of the Suoi Nghi | Floats | — | Qtz,Goe,Py dissemination | VAM 62 | — | < 2 | < 2 | < 0.001 | < 0.001 | < 0.001 | 0.002 | 0.017 | 0.007 | < 5 |
| Q7 | Lower reaches of the Suoi Nghi | Floats | Limestone ? | Qtz,Py dissemination | VAM 65 | — | < 2 | < 2 | < 0.001 | < 0.001 | < 0.001 | 0.002 | 0.017 | 0.010 | < 5 |
| Q8 | Ban Coi | Floats | Sandstone ? | Qtz,Cp? | VMM 55 | — | < 2 | < 2 | 0.456 | 0.017 | < 0.001 | 0.003 | 0.038 | 0.053 | < 5 |

Qtz:Quartz Py:Pyrite Goe:Goethite Cp:Chalcopyrite

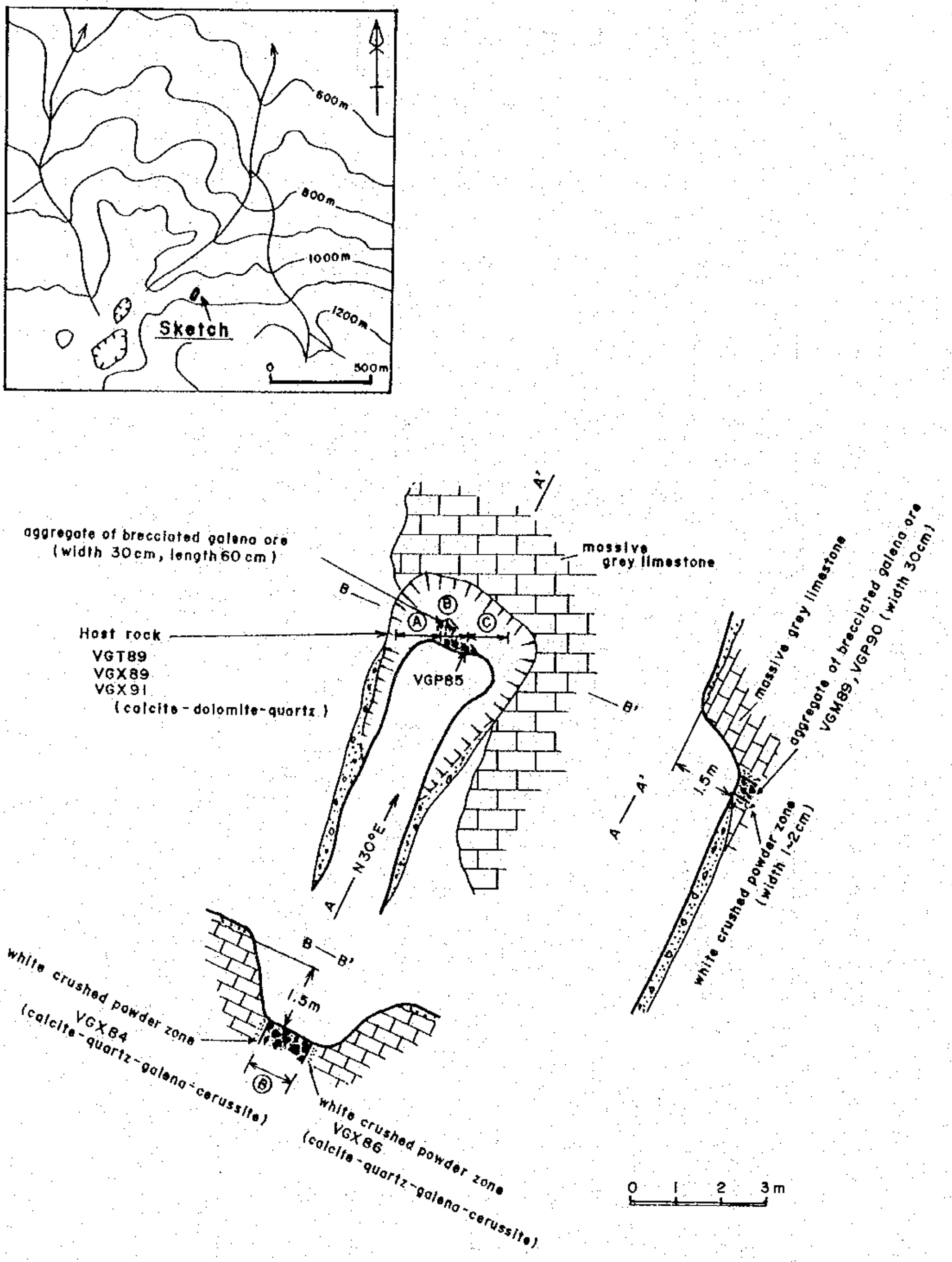


| Sample No. | wd. (m) | Au (ppb) | Ag (ppm) | Cu (%) | Pb (%) | Zn (%) | Ni (%) | Cr (%) | Mn (%) | Pt (ppb) |
|---|---|---|---|---|---|---|---|---|---|---|
| Ⓐ VGM82 | 1.0 | <2 | <2 | <0.001 | 0.713 | 0.002 | 0.001 | 0.002 | 0.007 | <5 |
| Ⓑ VGM87 | 0.6 | <2 | 53 | <0.001 | 8.861 | 0.012 | <0.001 | 0.016 | 0.007 | <5 |
| Ⓒ VGM83 | 1.0 | <2 | <2 | <0.001 | 0.019 | 0.010 | <0.001 | <0.001 | 0.012 | <5 |

Fig.Ⅲ-1-5 Geologic Sketch of the Suoi Can Mineral Showing

| Sample No. | Sampling width(m) | Au | Ag | Cu | Pb | Zn | Ni | Cr | Mn | Pt |
|---|---|---|---|---|---|---|---|---|---|---|
| VGM 82 | 1.0 | <2 | <2 | <0.001 | 0.713 | 0.002 | 0.001 | 0.002 | 0.007 | <5 |
| VGM 83 | 1.0 | <2 | <2 | <0.001 | 0.019 | 0.010 | <0.001 | 0.001 | 0.012 | <5 |
| VGM 87 | 0.6 | <2 | 53 | <0.001 | 8.861 | 0.012 | <0.001 | 0.016 | 0.007 | <5 |

Au and Pt are in ppb, Ag in ppm, and other elements in percent.

### 1.6.3. Platinum-copper-nickel mineralization

Abundant small ultramafic bodies intruded into a wide area from the western to eastern part of this survey area. This type of mineralization has been confirmed by GSV within 5 bodies located in the western and eastern parts of the area. The mineralization is characterized by the dissemination of very small metallic-mineral grains in ultramafic bodies. Therefore, it is not easy to clarify the details of mineralization grade in the field survey. Thus, in the course of this survey, samples for chemical analysis were collected from the ultramafic bodies or floats in case a small amount of very small metallic-mineral grains (chalcopyrite?) were discerned. The sampling was made at 14 localities in the whole survey area (Figure Ⅲ-1-4). The characteristics of the above 14 ultramafic rocks were summarized in Table Ⅲ-1-2 together with the assay results. The maximum platinum content is 40 ppb, and this revealed that the platinum mineralization is weak as far as collected samples are concerned.

### 1.6.4. Pyritization zone

Other than three types of mineralization reported above, twelve pyritization zones were found in the area (Figure Ⅲ-1-4). Most of the pyritization occur along fractures formed in Devonian sedimentary rocks and in the vicinity of the contact zones between ultramafic bodies and intruded sedimentary rocks. Although some pyritization zones are formed in a hydrothermal alteration zone of valuable mineral deposits, many zones have no genetic relation to the deposits. Therefore, pyritization itself can hardly be regarded as a significant mineralization unless there is evidence that the pyritization is accompanied by the valuable mineral deposits other than the above occurrence. (but in the case that pyrite occurs as high-grade massive ore, the ore sometimes can be minable.) Thus, in this description the presence of those pyritization zones is merely recorded for the field information. Table Ⅲ-1-3 shows the characteristics of the above pyritization zones together with assay results of collected samples.

Table Ⅲ-1-2 Assay Results of Ultramafic Rock Samples in the Van Yen Area

| No. | Sample locality | Occurrence | Host rock | Mineral assemblage | Sample No. | Dimensions & trend (m) | Ore grade Au ppb | Ag ppm | Cu % | Pb % | Zn % | Ni % | Cr % | Mn % | Pt ppb |
|---|---|---|---|---|---|---|---|---|---|---|---|---|---|---|---|
| UM 1 | Middle reaches of the Suoi Lang | Floats | Gabbro ? | — | VGM 60 | — | < 2 | < 2 | 0.007 | 0.002 | 0.047 | 0.010 | 0.012 | 0.161 | < 5 |
| UM 2 | Xom Lien | Intrusive | Gabbro ? | — | VSM 51 | N50W,10NE | < 2 | < 2 | 0.005 | < 0.001 | 0.018 | 0.034 | 0.112 | 0.143 | 5 |
| UM 3 | Suoi Can | Floats | Peridotite | — | VGM 52 | — | < 2 | < 2 | 0.010 | < 0.001 | 0.024 | 0.081 | 0.102 | 0.118 | 10 |
| UM4 | Suoi Can | Floats | Peridotite | — | VGM 93 | — | < 2 | < 2 | 0.005 | 0.197 | 0.026 | 0.114 | 0.169 | 0.103 | 15 |
| UM5 | Suoi Can | Floats | Peridotite | — | VGM 81 | — | < 2 | < 2 | 0.011 | < 0.001 | 0.026 | 0.133 | 0.167 | 0.108 | 10 |
| UM6 | Moung Do | Floats | Dunite | Cp,Mt | VAM 56 | — | < 2 | < 2 | 0.005 | < 0.001 | 0.052 | 0.111 | 0.108 | 0.136 | 15 |
| UM7 | Suoi Nho | Floats | Peridotite | — | VBM 54 | — | < 2 | < 2 | 0.008 | < 0.001 | 0.036 | 0.118 | 0.159 | 0.122 | 10 |
| UM8 | Suoi Duo | Intrusive | Dunite | — | VMM 54 | N50E? | < 2 | < 2 | 0.004 | 0.002 | 0.024 | 0.130 | 0.152 | 0.116 | 15 |
| UM9 | Muong Ban | Floats | Dunite | — | VBM 55 | — | < 2 | < 2 | 0.005 | < 0.001 | 0.031 | 0.111 | 0.133 | 0.115 | 10 |
| UM10 | Upper reaches of the Suoi Nghi | Intrusive | Dunite | — | H1-1 | — | < 2 | < 2 | 0.009 | 0.003 | 0.019 | 0.096 | 0.183 | 0.135 | 15 |
| UM11 | Upper reaches of the Suoi Nghi | Intrusive | Dunite | — | H2-2 | — | < 2 | < 2 | 0.017 | 0.002 | 0.005 | 0.052 | 0.245 | 0.088 | 40 |
| UM12 | Upper reaches of the Suoi Nghi | Intrusive | Dunite | — | H3-1 | — | < 2 | < 2 | 0.011 | 0.008 | 0.005 | 0.033 | 0.245 | 0.072 | 35 |
| UM13 | Upper reaches of the Suoi Nghi | Intrusive | Dunite | — | H4 | — | < 2 | < 2 | 0.055 | 0.002 | 0.005 | 0.044 | 0.231 | 0.072 | 35 |
| UM14 | Upper reaches of the Suoi Nghi | Intrusive | Dunite | — | H5 | — | < 2 | < 2 | 0.015 | 0.002 | 0.006 | 0.036 | 0.258 | 0.075 | 20 |

Cp:Chalcopyrite Mt:Magnetite

## Table Ⅲ-1-3 Characteristics of Pyritization Zones in the Van Yen Area

| No. | Sample locality | Occurrence | Host rock | Mineral assemblage | Sample No. | Dimensions & trend (m) | Ore grade Au ppb | Ag ppm | Cu % | Pb % | Zn % | Ni % | Cr % | Mn % | Pt ppb |
|---|---|---|---|---|---|---|---|---|---|---|---|---|---|---|---|
| P1 | Upper reaches of the Suoi Lang | Vein ? | Phyllitic shale | Goe,Py dissemination | VGM 63 | — | < 2 | < 2 | < 0.001 | 0.008 | 0.048 | 0.014 | 0.015 | 0.409 | < 5 |
| P2 | Muong Do | Gossan | Limestone ? | Qtz,Goe | VAM 57 | — | < 2 | < 2 | < 0.001 | 0.026 | 0.201 | 0.019 | 0.039 | 0.178 | < 5 |
| P3 | Muong Do | Vein | Phyllitic mudstone | gossan | VMM 52 | N84E ,69N wd=0.2-0.3 | < 2 | < 2 | < 0.001 | 0.002 | 0.005 | 0.001 | 0.030 | 0.003 | < 5 |
| P4 | Muong Do | Vein | Phyllitic mudstone | Py dissemination | VMM 53 | N82E ,84N wd=3.0 | < 2 | < 2 | < 0.001 | 0.004 | 0.019 | 0.003 | 0.030 | 0.009 | < 5 |
| P5 | Middle reaches of the Suoi Tioun | Dissemination | Limestone (contact part with ultra-maffic rock) | Py dissemination | VAM 58 | 0.2 wd | < 2 | < 2 | 0.012 | < 0.001 | < 0.001 | < 0.001 | < 0.001 | 0.030 | < 5 |
| P6 | Middle reaches of the Suoi Tioun | Dissemination | Limestone (contact part with ultra-maffic rock) | Cp,Po,Py dissemination | VAM 59 | 0.2 wd | < 2 | < 2 | 0.007 | < 0.001 | < 0.001 | < 0.001 | < 0.001 | 0.026 | < 5 |
| P7 | Upper reaches of the Suoi Tion | Dissemination | Mudstone | Po,Py dissemination | VAM 60 | — | < 2 | < 2 | < 0.001 | 0.002 | 0.018 | 0.003 | 0.004 | 0.056 | < 5 |
| P8 | Upper reaches of the Suoi Tion | Dissemination | Dolerite | Po,Py dissemination | VAM 61 | — | < 2 | < 2 | 0.001 | < 0.001 | 0.034 | 0.006 | 0.044 | 0.109 | < 5 |
| P9 | Upper reaches of the Suoi Nghi | Floats | Limestone ? | Py dissemination | VAM 64 | — | < 2 | < 2 | < 0.001 | < 0.001 | <0.001 | 0.002 | 0.021 | 0.003 | < 5 |
| P10 | Song Da | Dissemination | Limestone | Py dissemination | VAM 66 | — | < 2 | < 2 | < 0.001 | 0.002 | 0.001 | 0.002 | 0.015 | 0.029 | < 5 |
| P11 | Song Da | Dissemination | Mudstone | Py dissemination | VAM 67 | wd = 0.1-0.2m | < 2 | < 2 | 0.002 | 0.003 | 0.014 | 0.002 | 0.006 | 0.025 | < 5 |
| P12 | Lower reaches of the Suoi Lai | Floats | Sandstone | Py dissemination | VAM 68 | — | < 2 | < 2 | < 0.001 | < 0.001 | 0.004 | < 0.001 | 0.017 | 0.153 | < 5 |

Goe:Goethite  Py:Pyrite  Qtz:Quartz  Cp:Chalcopyrite  Po:Pyrrhotite

## CHAPTER 2. REGIONAL GEOCHEMICAL EXPLORATION

### 2.1. Stream Sediment Geochemical Exploration

#### 2.1.1. Objectives

Stream sediment geochemistry was carried out aiming to extract promising areas for mineral deposit based on geochemical characteristics of the regional survey area.

#### 2.1.2. Sampling and chemical analysis

About 100 g of stream sediments with under 80 mesh size were collected for stream sediment geochemistry sample. A number of samples is 915 in total. Samples were sieved into under 80 mesh fraction in the field and were sent to the laboratory (the Geoscience Laboratory of Bishimetal Exploration Co., Ltd.) for chemical analysis after drying. Samples were analyzed for nine elements of Au, Ag, Cu, Pb, Zn, Ni, Cr, As, and Hg. Localities of samples are shown in Plate 8. Analytical methods used and detection limits are shown below.

**Analytical Methods and Detection Limits**

| Element | Digestion and Methods | Detection Limits |
|---|---|---|
| Au | AAS | 1 ppb |
| Ag | AAS | 0.02 ppm |
| Cu | ICP | 0.2 ppm |
| Pb | ICP | 0.5 ppm |
| Zn | ICP | 1 ppm |
| Ni | ICP | 1 ppm |
| Cr | ICP | 1 ppm |
| As | ICP | 0.2 ppm |
| Hg | CV-AAS | 10 ppb |

AAS: Atomic Absorption Spectrometry
ICP: Inductivity Coupled Prasma Emission Spectrometry
CV-AAS: Cold Vapor Atomic Absorption Spectrometry

#### 2.1.3. Statistical data-processing

(1) Elemental statistics

Analytical values of each element are recorded in Appendix 6. Elemental statistics parameters calculated by anti-logarithm and common logarithm for analytical values are shown in Table Ⅲ-2-1. On the occasion of values below the detection limit, one half of detection limit values were substituted.

(2) Frequency distribution

Generally, in the case that analytical values follow normal or log-normal distribution, these values are considered to belong to single population. On the contrary, patterns deviate from normal or log-normal distribution in the case of composite population which consists of mixture of two or more dissimilar populations (for instance; background + anomaly originated in mineralization; Otsu et al., 1983).

Histograms of analytical values of each element drawn by logarithm are shown in Figure Ⅲ-2-1. Histograms of four elements Cu, Pb, Zn, and Hg follow log-normal distribution, while those of the rest of elements do not follow normal or log-normal distribution, namely, elements Au, Ag, and As of which most of values are below the detection limit show the L-shape pattern and elements Ni and Cr show the pattern with double frequency peaks.

(3) Correlation among elements

Correlation coefficients and correlation diagrams are shown in Table Ⅲ-2-2 and Figure Ⅲ-2-2, respectively. The following 6 pairs show significant correlation coefficient.

Ni-Zn (R=0.8853), Ni-Cr (R=0.8654), Ni-Cu (R=0.7985)
Zn-Cr (R=0.7926), Cu-Zn (R=0.7799), Cu-Cr (R=0.6375)

2.1.4. Geochemical anomalies and anomalous zones

(1) Determination of threshold value

In order to determine threshold values, Lepelitier's method (1969) with cumulative frequency distribution diagrams drawn by logarithm of analytical values was adopted.

Cumulative frequency distribution diagrams of each element were drawn on logarithmic probability graph paper (Figure Ⅲ-2-3).

Diagrams of three elements Cu, Zn, and Hg of which histograms show log-normal distribution indicate rectilineal pattern, so that these values are considered to belong to single population. Therefore, the values of mean value + standard deviation x 2 ($m+2\sigma$) are used for threshold values of these elements to check higher grade parts.

As for Au, values of 96 % of samples are below the detection limit, and distribution pattern itself is indistinct. Therefore the detection limit is treated as threshold value.

Diagrams of Ag, Pb, and As show breaking points around probability 1 %. Therefore, values at these points are used for threshold values of these elements. However, it is uncertain whether the breaking point indicates

Table Ⅲ-2-1 Elemental Statistics Parameters in Stream Sediment Geochemistry of the Van Yen Area

| Antilog | Au | Ag | Cu | Pb | Zn | Ni | Cr | As | Hg |
|---|---|---|---|---|---|---|---|---|---|
| Minimum | 0.5 | 0.01 | 1.8 | 0.25 | 5 | 2 | 0.5 | 0.1 | 5 |
| Maximum | 313 | 3.03 | 638.4 | 714.1 | 1,969 | 2,368 | 18,984 | 72.4 | 778 |
| Average (m) | 1.2 | 0.21 | 20.2 | 18.1 | 77 | 55 | 601 | 3.6 | 63 |
| Standard deviation (σ) | 11.0 | 0.27 | 23.8 | 32.1 | 88 | 103 | 1,160 | 5.0 | 71 |
| PLDL*1 | 96.4% | 36.9% | 0.0% | 0.3% | 0.1% | 0.3% | 9.1% | 33.0% | 3.5% |

*1 : Percentage of less than detection limit

| Log | Au | Ag | Cu | Pb | Zn | Ni | Cr | As | Hg |
|---|---|---|---|---|---|---|---|---|---|
| Minimum | -0.301 | -2.000 | 0.255 | -0.602 | 0.699 | 0.301 | -0.301 | -1.000 | 0.699 |
| Maximum | 2.496 | 0.481 | 2.805 | 2.854 | 3.294 | 3.374 | 4.278 | 1.860 | 2.891 |
| Average (m) | -0.268 | -1.141 | 1.211 | 1.149 | 1.744 | 1.470 | 1.937 | 0.061 | 1.648 |
| *Antilog* | *0.5* | *0.07* | *16.2* | *14.1* | *56* | *30* | *87* | *1.2* | *45* |
| Standard deviation (σ) | 0.213 | 0.723 | 0.281 | 0.285 | 0.347 | 0.470 | 1.077 | 0.808 | 0.356 |

Table Ⅲ-2-2 Correlation Coefficients between Element Pairs in Stream Sediment Geochemistry of the Van Yen Area

| | Au | Ag | Cu | Pb | Zn | Ni | Cr | As | Hg |
|---|---|---|---|---|---|---|---|---|---|
| Au | 1 | | | | | | | | |
| Ag | 0.004 | 1 | | | | | | | |
| Cu | 0.056 | 0.150 | 1 | | | | | | |
| Pb | -0.032 | 0.077 | 0.402 | 1 | | | | | |
| Zn | 0.049 | 0.167 | **0.780** | 0.418 | 1 | | | | |
| Ni | 0.053 | 0.216 | **0.798** | 0.260 | **0.885** | 1 | | | |
| Cr | 0.050 | 0.090 | **0.638** | 0.116 | **0.793** | **0.865** | 1 | | |
| As | 0.000 | 0.263 | 0.186 | 0.287 | 0.126 | 0.123 | 0.012 | 1 | |
| Hg | 0.044 | 0.087 | 0.187 | 0.254 | 0.248 | 0.211 | 0.146 | 0.173 | 1 |

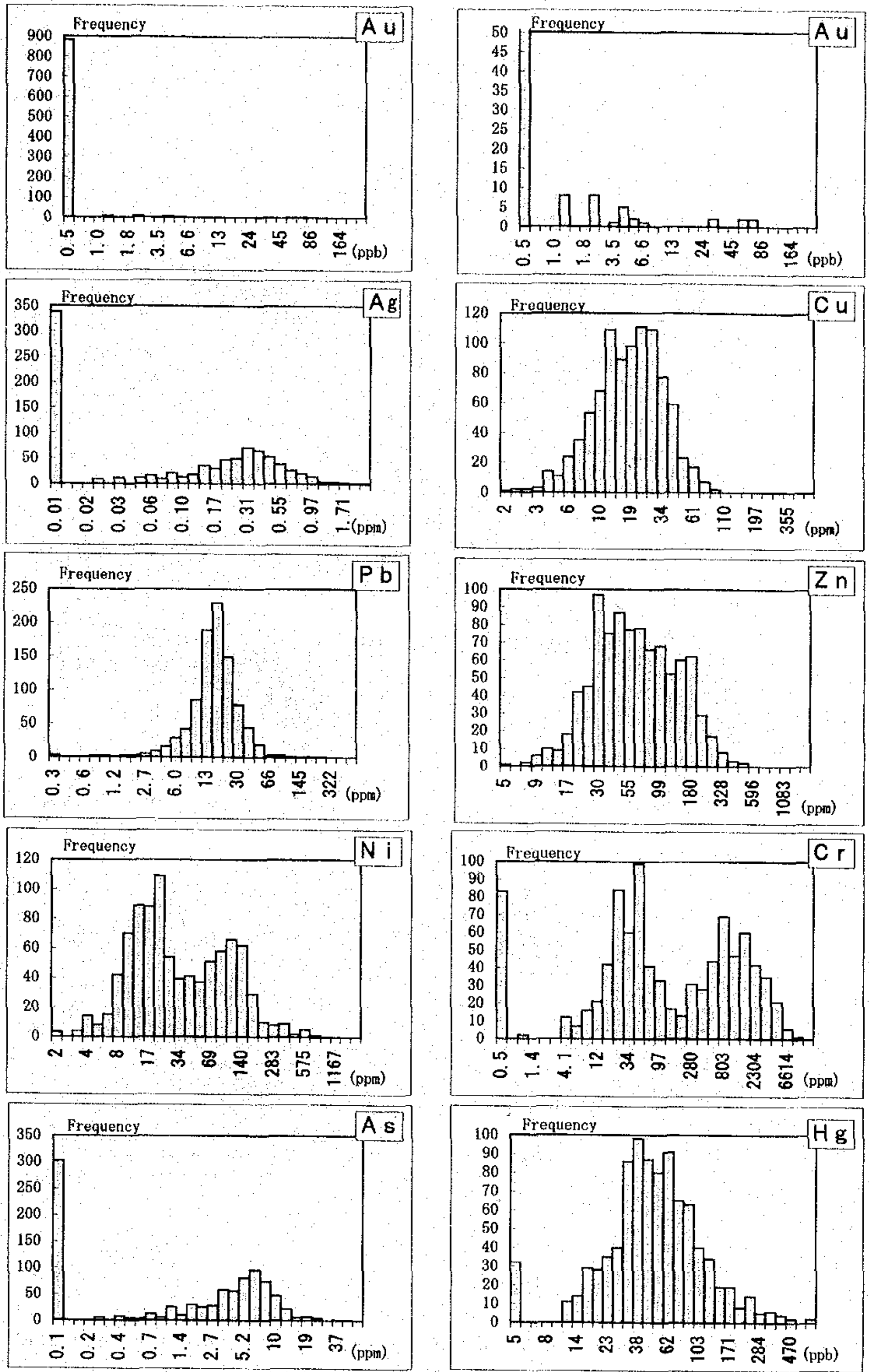


**Fig.Ⅲ-2-1 Histograms of Assays on Stream Sediment Geochemical Samples Collected in the Van Yen Area**

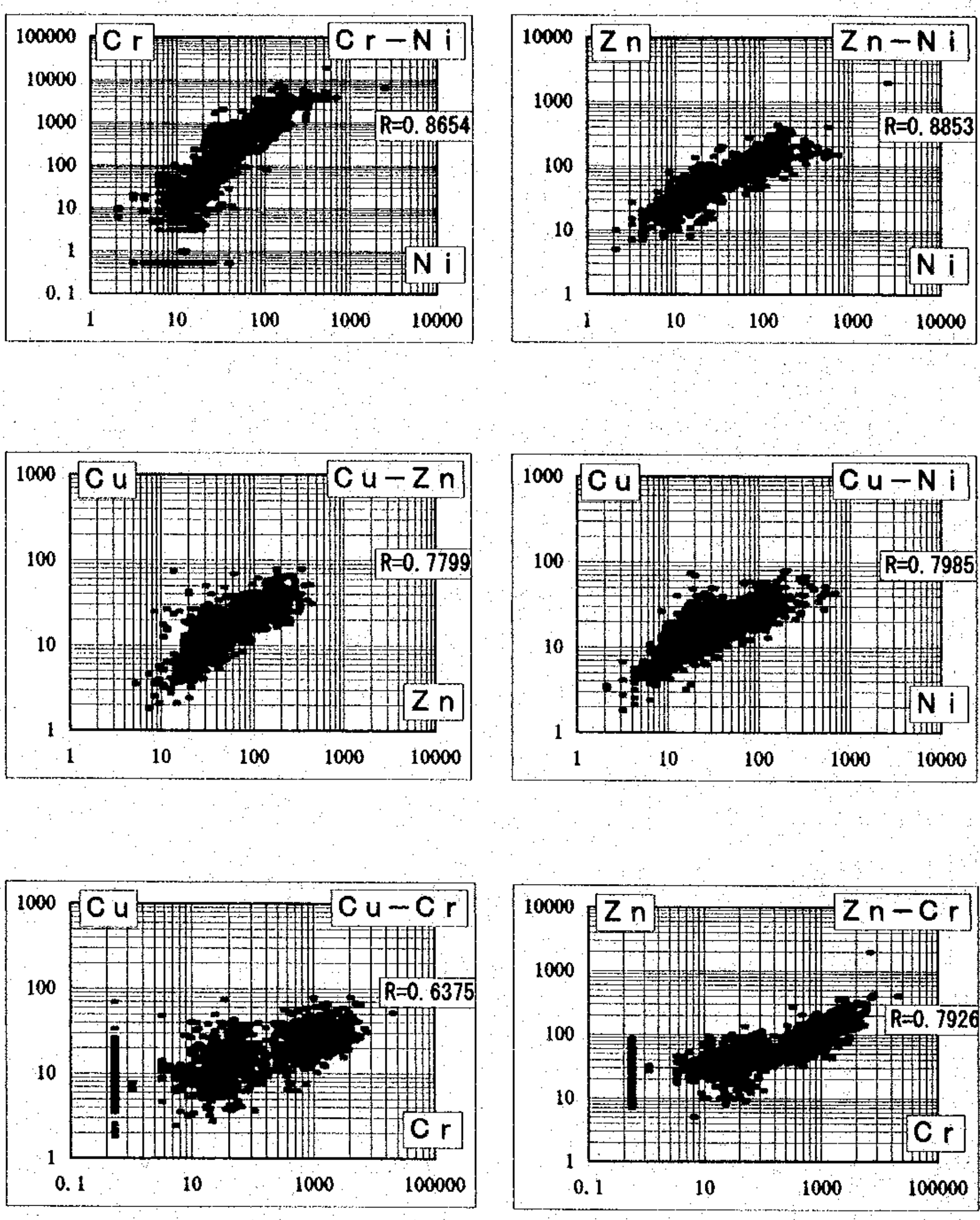


Fig.Ⅲ-2-2 Correlation Diagram between Element Pairs on Stream Sediment Geochemical Samples Collected in the Van Yen Area

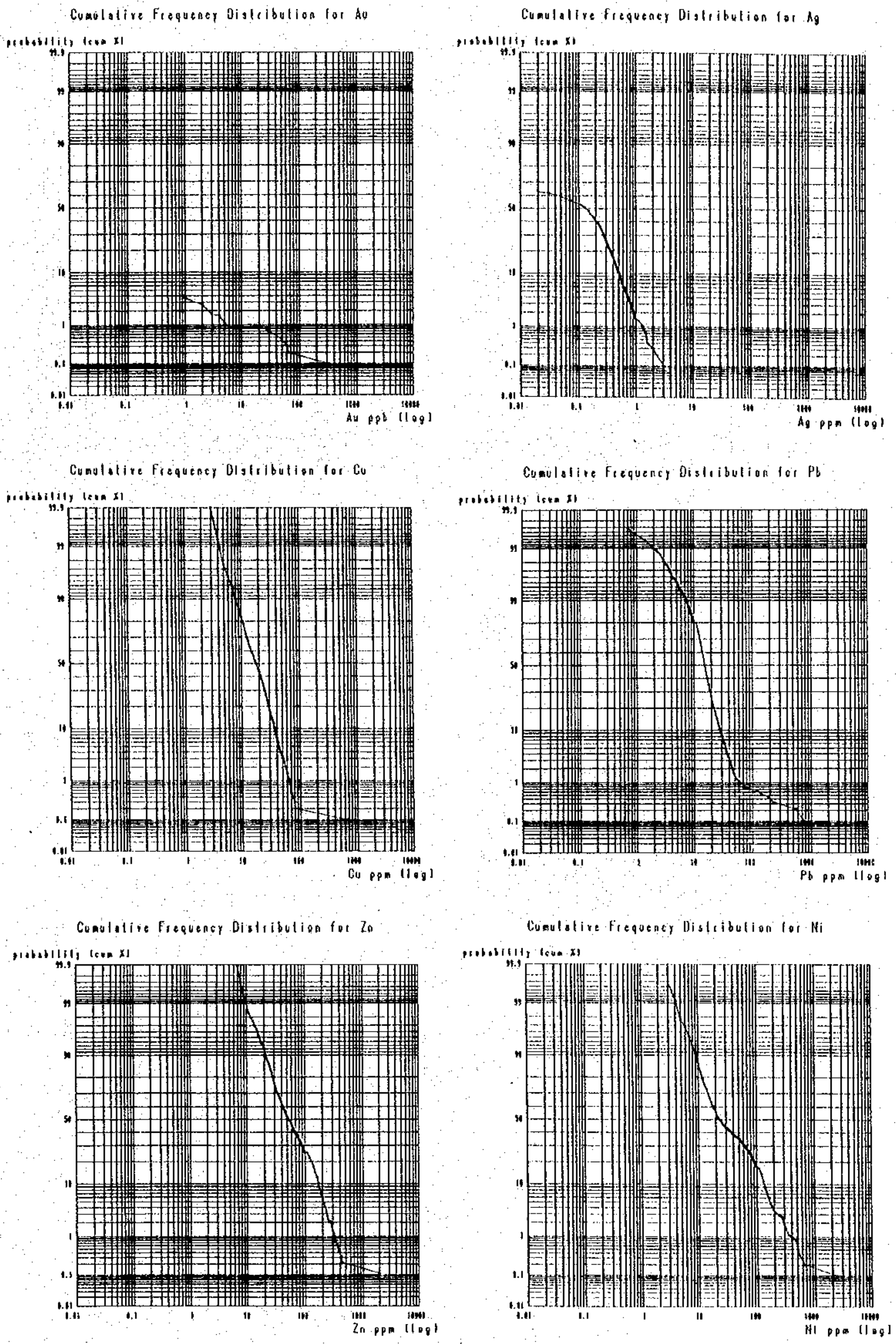


Fig. Ⅲ-2-3 Cumulative Frequency Distribution of Assays on Stream Sediment Geochemical Samples Collected in the Van Yen Area (1)

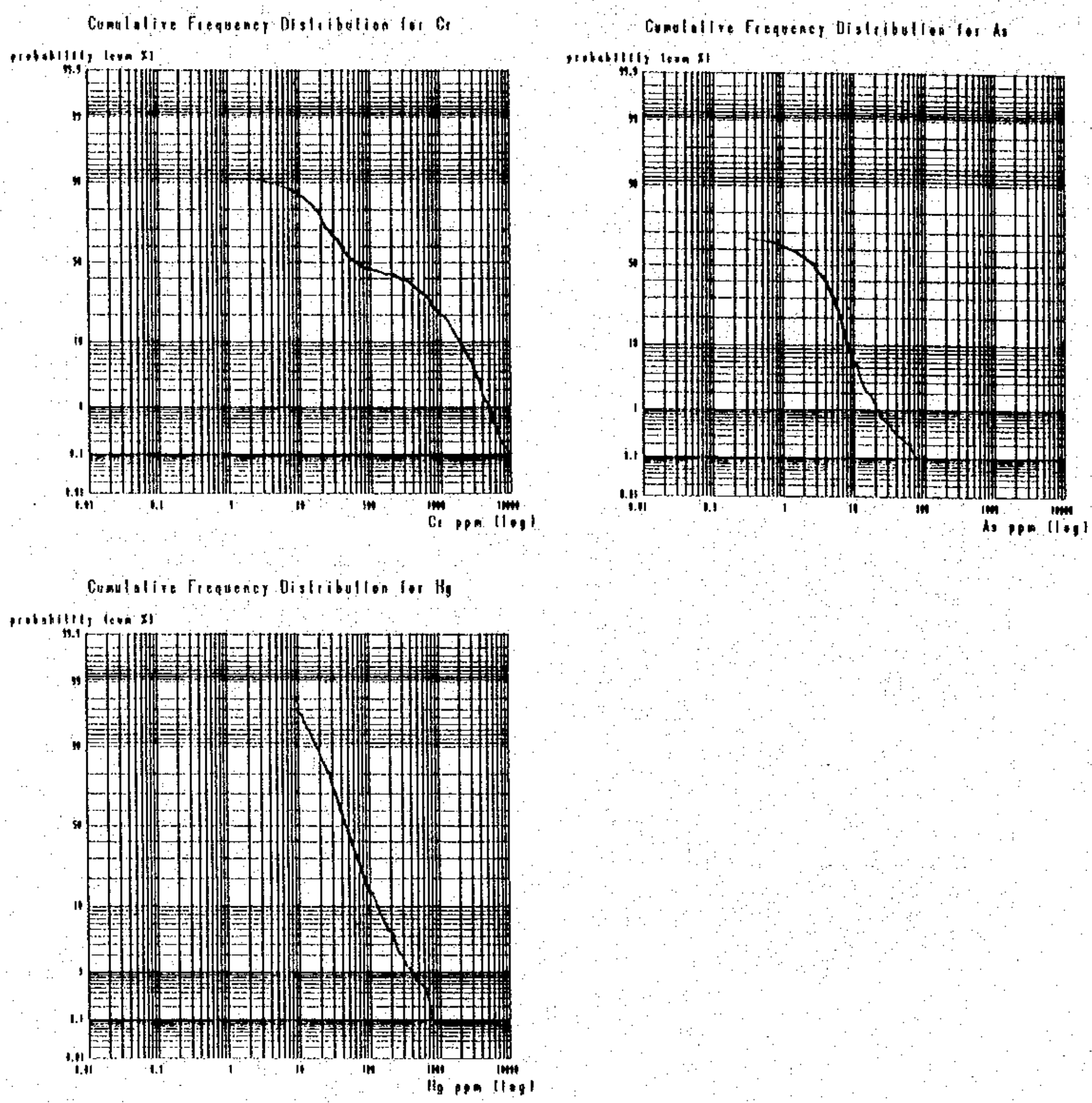


Fig.Ⅲ-2-3 Cumulative Frequency Distribution of Assays on Stream Sediment Geochemical Samples Collected in the Van Yen Area (2) disparity of populations or not, because differences of inclination are slight and number of samples separated by the breaking point around probability 1 % are insufficient.

On the other hand, diagrams of Ni and Cr of which histograms have double frequency peaks show S-shape curve and indicate these values belong to typical composite population. As for these two elements, the values at point of minimum frequency between two peaks are used for threshold values.

Based on the above threshold values, the following anomalies were instituted.

Au: weak anomaly (≥1 ppb, <10 ppb)
strong anomaly (≥10 ppb)
Ag: anomaly (≥1 ppm)
Cu: anomaly (≥59.2 ppm)
Pb: anomaly (≥60.0 ppm)
Zn: anomaly (≥273.6 ppm)
Ni: weak anomaly (≥45 ppm, <90 ppm)
; value at point of minimum frequency between two peaks
medium anomaly (≥90 ppm, <257 ppm)
; value at righthand frequency peak
strong anomaly (≥257 ppm); $m+2\sigma$
Cr: weak anomaly (≥200 ppm, <1,000 ppm)
; value at point of minimum frequency between two peaks
medium anomaly (≥1,000 ppm, <4,000 ppm)
; value at righthand frequency peak
strong anomaly (≥4,000 ppm)
; 2.5 % of the whole analytical values
As: anomaly (≥20 ppm)
Hg: anomaly (≥229.0 ppb)

(2) Anomalous zones

Anomalous points of each element extracted on the basis of the above threshold values are plotted in Appendix 12. Here anomalous zone includes weak to strong anomalous zone unless noted.

Areas with concentration of anomalous points are listed for each element hereunder. In principle, concentration means cases with nearby (about 1 km) two points or with 3 or more points closely (3 to 4 km) distributed.

Au:

a) Northwestern part of the area; around 10 km west of Thu Cuc
b) Western part of the area; around 5 km south of Ban Suoi Hang
c) Southeastern part of the area; around 5 km north of Ben Khe
d) Southeastern part of the area; around Ben Khe

Ag:

a) Northwestern part of the area; around 12 km west of Thu Cuc; south of the Au anomalous zone a)
b) Western part of the area; around Ban Suoi Hang
c) Central part of the area; around 4 km southeast of Lang Phat
d) Southeastern part of the area; around 5 km north of Ben Khe; corresponding to Au anomalous zone c)

Cu:

a) Western part of the area; around 3 km south of Ban Suoi Hang
b) Central part of the area; around 7 km southwest of Lang Phat
c) Southeastern part of the area; around 5 km north of Ben Khe; corresponding to Au anomalous zone c) and Ag anomalous zone d)

Pb:

a) Northwestern part of the area; around 10 km west of Thu Cuc

Zn:

a) Northwestern part of the area; around 10 km west of Thu Cuc; corresponding to Pb anomalous zone a)
b) Central part of the area; around 5 km southeast of Lang Phat

Ni:

a) Central part of the area; strong anomaly concentration around 7 km southwest of Lang Phat
b) Western part of the area; strong anomalous part around 5 km south of Ban Suoi Hang
c) North to central part of the area; weak to medium anomalous zone widely extended NW-SE
d) Central part of the area; medium anomalous zone around 12 km north-northwest of Ben Khe

Cr:

a) Central part of the area; strong anomalous zone around 7 km southwest of Lang Phat; corresponding to Ni strong anomalous zone a)
b) Western part of the area; strong to medium anomalous zone around 5 km south of Ban Suoi Hang; corresponding to Ni strong anomalous zone b)
c) Eastern part of the area; strong to medium anomalous zone around 4

km southeast of Lang Phat; corresponding to Ag anomalous zone c)

d) North to central part of the area; weak to medium anomalous zone widely extended NW-SE

e) Central part of the area; weak to medium anomalous zone around 12 km north-northwest of Ben Khe

As:

a) Southwestern part of the area; around 3 km southeast of Da May (No other clear concentration was revealed and anomalous points tend to scatter in the south in contrast to Ni and Cr distribution.)

Hg:

a) Northeastern part of the area; around 8 km northeast of Thu Cuc

b) Northeastern part of the area; around 2 km northeast of Thu Cuc

(3) Multivariate analysis

Principal component analysis was adopted in order to condense meaning of analytical values and to simplify interpretation of analytical values and correspondence with geology and mineralization. Then principal components 1, 2 and 3 were examined, because these eigenvalues are over 1.0 (this value is considered to be meaningful statistically). Values of eigenvector, factor loading, proportion, and cumulative proportion are shown in Table Ⅲ-2-3.

**Table Ⅲ-2-3 Results of Principal Components Analysis in Streem Sediment Geochemistry of the Van Yen Area**

| | Principal Component 1 | | Principal Component 2 | | Principal Component 3 | |
|---|---|---|---|---|---|---|
| | Eigenvector | Factor loading | Eigenvector | Factor loading | Eigenvector | Factor loading |
| Au | 0.037 | 0.070 | 0.079 | 0.092 | 0.938 | 0.942 |
| Ag | 0.134 | 0.258 | -0.375 | -0.439 | 0.232 | 0.233 |
| Cu | 0.455 | 0.874 | 0.043 | 0.051 | -0.039 | -0.040 |
| Pb | 0.243 | 0.468 | -0.429 | -0.502 | -0.221 | -0.222 |
| Zn | 0.489 | 0.940 | 0.103 | 0.120 | -0.046 | -0.046 |
| Ni | 0.489 | 0.941 | 0.173 | 0.202 | 0.006 | 0.006 |
| Cr | 0.434 | 0.835 | 0.323 | 0.378 | 0.002 | 0.002 |
| As | 0.129 | 0.249 | -0.633 | -0.741 | 0.075 | 0.075 |
| Hg | 0.175 | 0.336 | -0.350 | -0.410 | 0.086 | 0.086 |
| Eigen*1 | 3.695 | | 1.371 | | 1.008 | |
| Prop*2 | 0.411 | | 0.152 | | 0.112 | |
| Cum Pr*3 | 0.411 | | 0.563 | | 0.675 | |

*1 : Eigenvector *2 : Proportion *3 : Cumulative proportion

【Principal component 1】

Values of factor loading for Cu, Zn, Ni, and Cr are high positive of around 0.9, and value for Pb is next higher positive. There is no correlation between principal component 1 and elements Au, Ag, As, and Hg.

【Principal component 2】

Value of factor loading for As is relatively high negative, and values for Ag, Pb, and Hg are next higher negative. It is considered that elements except Au are extracted among the elements which have no correlation with principal component 1. However, there is no significant correlation among these 4 elements (see Table Ⅲ-2-2).

【Principal component 3】

Values of factor loading for Au and Ag are positive. It is considered that information about Au, which is not extracted in relation to principal component 1 or 2, is brought.

In order to investigate distribution of information about principal components, sampling points with high factor score are plotted on the basis of the following threshold values (Appendix 13).

| | remarked elements | threshold values |
|---|---|---|
| Principal component 1 | Cu, Zn, Ni, Cr | $m+1\sigma$ , $m+2\sigma$ |
| Principal component 2 | As, Hg, Pb | $m-1\sigma$ , $m-2\sigma$ |
| Principal component 3 | Au, Ag | $m+1\sigma$ , $m+2\sigma$ |

Principal component 1 :

Points with factor score over $m+1\sigma$ are distributed in one zone extending widely NW-SE from northern to central part of the area (same pattern with Ni and Cr anomalous zones) and another zone extending NW-SE from around 5 km south of Ban Suoi Hang to around 12 km north-northwest of Ben Khe. Points with factor score over $m+2\sigma$ are distributed in zone around 7 km southwest of Lang Phat.

Principal component 2 :

Points with factor score over $m-1\sigma$ are distributed mainly in central to southern part of the area. No concentration is observed for points with factor score over $m-2\sigma$ .

Principal component 3 :

Since the greater part of factor score comes out from Cu, the results are almost same as Au anomaly map.

2.1.5. Consideration

(1) Results of analysis and statistics

In relation to 9 elements analyzed in the second phase exploration, an average composition of elements concerned in the earth's crust and principal rocks are shown in the table below.

| Element | Earth's crust | Ultra mafic rocks | Mafic rocks | Granite | Lime-stone | Sand-stone | Shale |
|---|---|---|---|---|---|---|---|
| Au(ppb) | 4 | 3.2 | 3.2 | 2.5 | 5 | 5 | 4 |
| Ag(ppb) | 70 | 60 | 100 | 37 | 100 | 250 | 190 |
| Cu(ppm) | 55 | 42 | 72 | 12 | 5 | 10 | 42 |
| Pb(ppm) | 13 | 1 | 4 | 18 | 5 | 10 | 25 |
| Zn(ppm) | 70 | 58 | 94 | 51 | 21 | 40 | 100 |
| Ni(ppm) | 75 | 2000 | 130 | 4-5 | 20 | 2 | 68 |
| Cr(ppm) | 100 | 1980 | 170 | 4.1 | 11 | 35 | 90 |
| As(ppm) | 1.8 | 1.0 | 1.5 | 2.1 | 1.1 | 1.2 | 12 |
| Hg(ppb) | 80 | 4 | 10 | 40 | 40 | 30 | 20-400 |

Although the above average composition cannot be compared directly with geochemical contents, some studies were done for reference as in the following. Since the area is mainly underlain by limestone, sandstone and shale with granitic intrusives and small ultramafic bodies, correlation with figures for these rocks were carried out hereunder.

Element with threshold values for strong anomaly being ten times or more of the average composition (maximum value of each element except value of the ultramafic rocks due to small dimensions) is only Cr. Histogram of Cr shows pattern with double frequency peaks and these values seem to belong to two populations as stated before. Numbers of values in each population are approximately in the ratio of 60 % : 40 % and mean values are about 50 ppm and 1,600 ppm, respectively.

Threshold values of other elements are merely one to three times of the average composition. Consequently, it is hard to mention that geochemical anomalies of these elements have originated in mineralization.

(2) Relationship with geology and geologic structure

Values of Cr, Ni, Cu, and Zn tend to be high in the zone extending NW-SE from northern to central part of the area. Ultramafic rocks can be pointed out as rocks with high values of these elements. However, Devonian $D_1$ and $D_2$ mudstones without large ultramafic bodies are developed in the zone on the correspondence of high values and geologic map. The Cr values exceed 1,000 ppm at points in almost all small tributaries in the zone, and no ultramafic float was observed in these tributaries. From these, it follows that it is rather reasonable to consider the $D_1$ and $D_2$ mudstones themselves are rich in Ni and Cr than to think there is a lot of ultramafic bodies intruded into the $D_1$ and $D_2$ mudstone. Furthermore, values of Ni and Cr are also high in the zone extending from western to central part of the area, and this zone also corresponds with distribution of the Devonian $D_1$ and $D_2$ mudstones. Many points with high Cr values are observed in the area covered by the CP (Carboniferous to Permian) limestone in the central part of the area, it can be considered that these high values are brought from upper reaches where $D_1$ and $D_2$ mudstones are developed.

Points with especially high Ni and Cr values are revealed around 7 km southwest of Lang Phat and around 5 km south of Ban Suoi Hang. It seems that these values are influenced by ultramafic rocks located in the upper reaches. The same results mentioned above are taken in the factor score map of principal component 1.

## 2.2. Panned Concentrate Geochemical Exploration

(1) Objectives

The gold, lead-zinc, and platinum-copper-nickel mineralization represented by the Suoi Can mineral showing and others was confirmed by the previous geologic and metallogenic data in this regional survey area. This exploration was carried out in the survey area in order to evaluate the characteristics of heavy minerals in the mineralization zones and to discover new potential areas.

(2) Collection, treatment, and identification of panned concentrates

The sampling of panned concentrates was carried out along the main streams and their tributaries, and at the streams around the known mineralization zones during the course of the regional geological survey. The total number of panned concentrates is 240 samples in this area. Each sample was collected by five-times panning (approximately 25ℓ). The samples were dried up and weighed. The heavy minerals were identified based on the method shown in Figure Ⅲ-2-4.

(3) Results of the mineral identification

The results of the mineral identification are laid out in Appendix 8. The identified minerals are magnetite, ilmenite, limonite, hematite, garnet, staurolite, epidote, siderite, tourmaline, chromite, pyroxene, serpentine, zircon, rutile, cinnabar, pyrite, and native gold. The heavy minerals related to mineralization in this area are considered to be native gold and chromite.

The number of their localities is as follows.

- Gold: 9
- Chromite: 41

The heavy minerals of magnetite, ilmenite, limonite, hematite, epidote, tourmaline, zircon, and rutile were usually observed in this area.

(4) Distribution of heavy minerals

The localities of heavy minerals confirmed microscopically for native gold and chromite are shown in Figure Ⅲ-2-5 and described below.

【Native gold】

1) Upper reaches of the Mua River, 4 km west of Thu Cuc
2) Tributary of the Mua River, 8.5 km west of Thu Cuc
3) Lower reaches of the Mua River, about 20 km southeast of Thu Cuc
4) Middle reaches of the Can Stream
5) Upper reaches of the Can Stream
6) Tributary of the Nuoc Thang Stream, 1 km west of Xom Nuoc Thang
7) Upper reaches of the Nghi Stream, tributary of the Khoang Stream
8) Middle reaches of the Neng Stream, tributary of the Da River, 1 km east of Ban Coi
9) The southeastern end of the area (on the left bank of the Da River)

【Chromite】

1) Middle reaches of the Mua River, 3 km west of Thu Cuc; 4 localities
2) Upper reaches of the Mua River, 8 km west of Thu Cuc; 7 localities
3) Upper reaches of the Khac Stream, 7 km southwest of Thu Cuc; 2 localities
4) In the vicinity of Kiet Son, lower reaches of the Mua River; 9

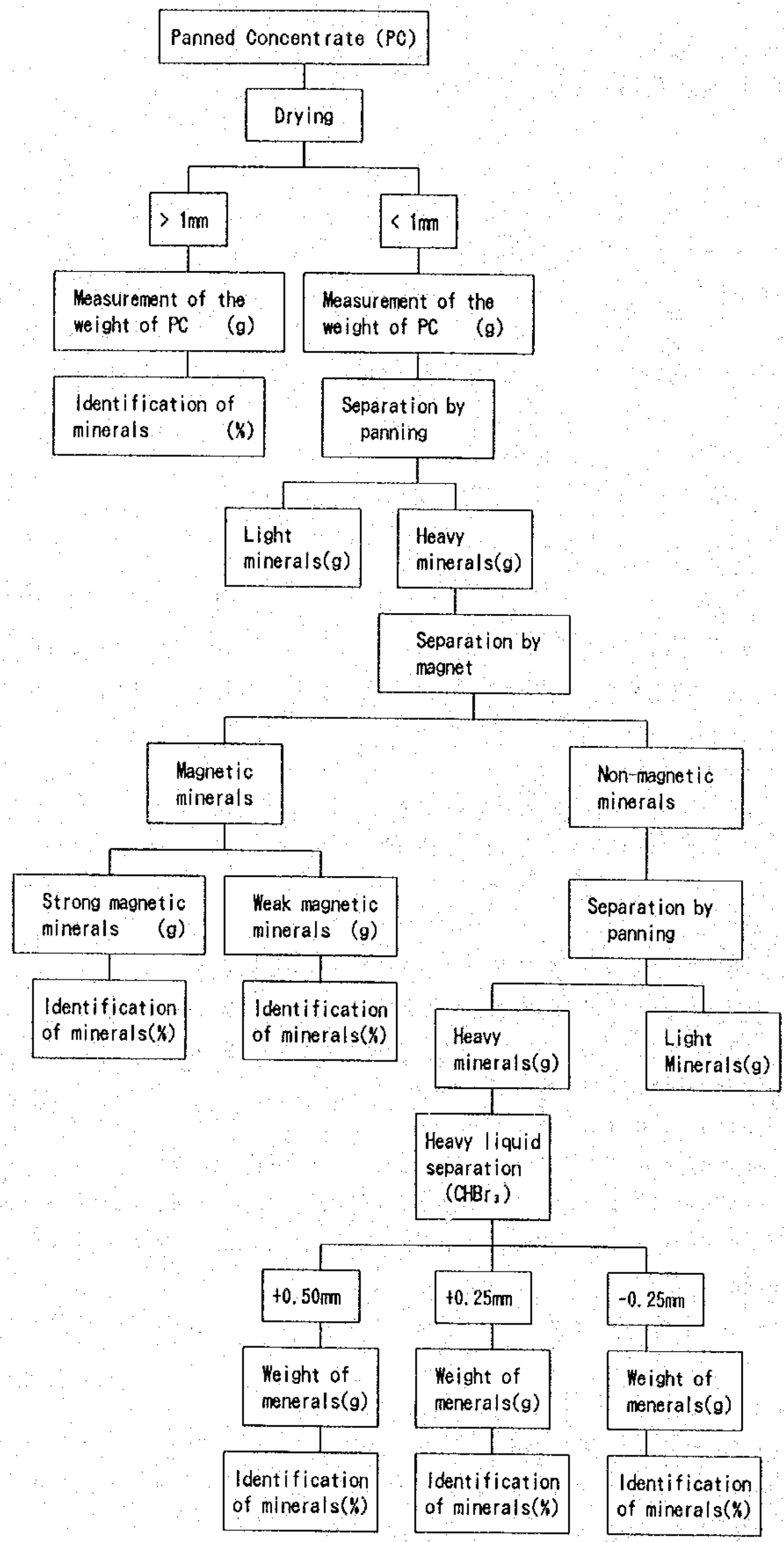


**Fig.Ⅲ-2-4 Flow Chart of the Methods for Identification of Heavy Minerals**

localities

5) Middle reaches of the Can Stream; 3 localities
6) Tributary of the upper reaches of the Mua River; 5 localities
7) Middle reaches of the Nuoc Thang Stream; 3 localities
8) Middle reaches of the Duo Stream, tributary of the Khoang Stream; 2 localities
9) Upper reaches of the Nghi Stream; 3 localities
10) Other localities

(5) Discussion

The following relationship was recognized between the localities of heavy minerals and the geology.

Native gold grains are sparsely confirmed in the whole survey area and their localities seem not to be related to the specified geologic units. Nevertheless, in three localities, 3), 7), and 8) mentioned above, stockwork of quartz or floats of vein quartz were found in the upper reaches of the streams of those localities. Thus, it seems possible that the gold grains derive from the stockwork or floats.

Most of chromite grains were confirmed in the lower reaches of the streams where ultramafic bodies are exposed. Thus, the origin of those minerals is considered to be controlled by the ultramafic intrusion. In other localities the ultramafic bodies were not recognized through the field survey. However, it is inferred that the bodies will occur in the upper reaches of the streams of the localities and they are the origin of the minerals.

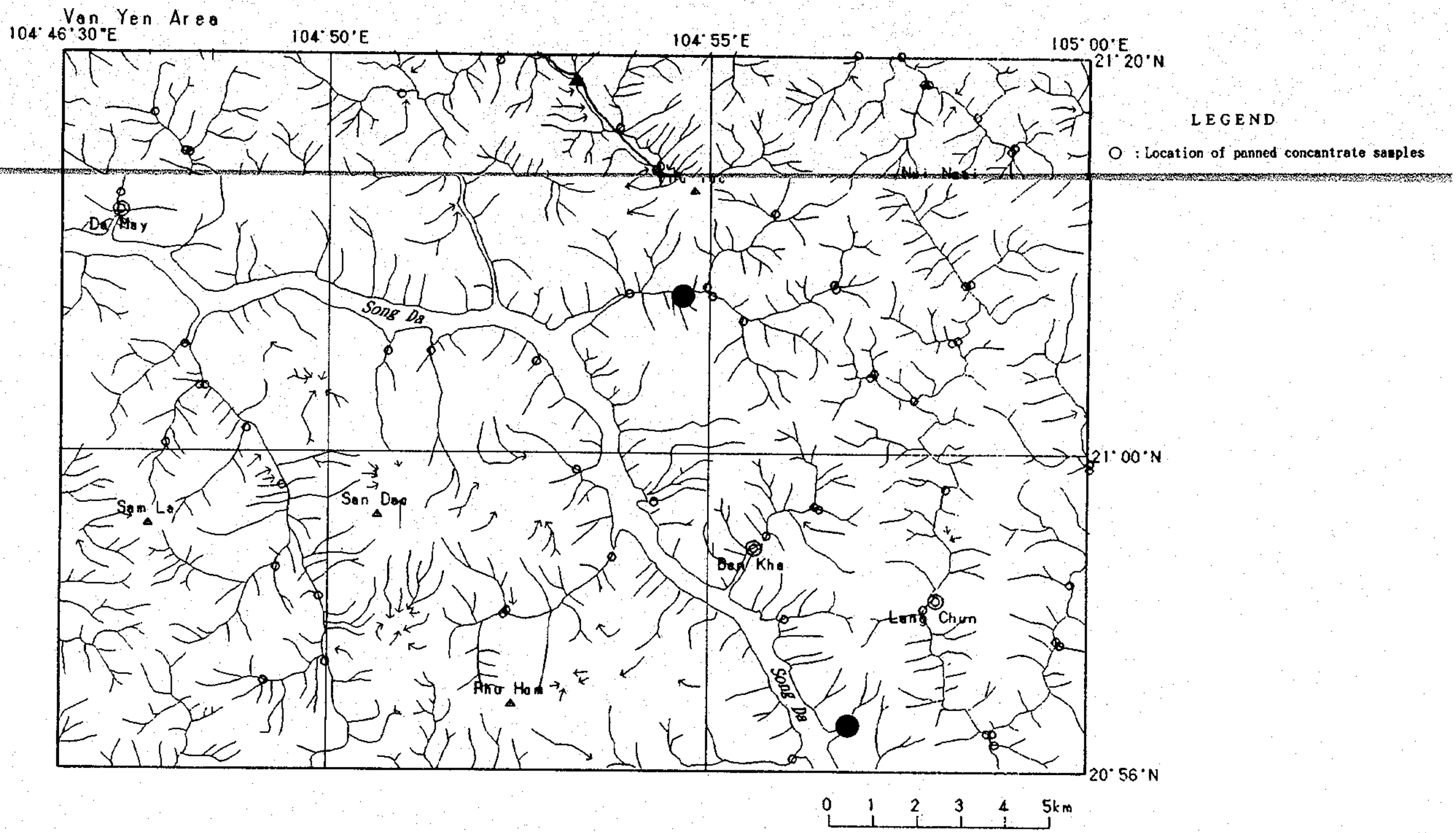


Fig.Ⅲ-2-5 Locality Map of Heavy Minerals in the Van Yen Area

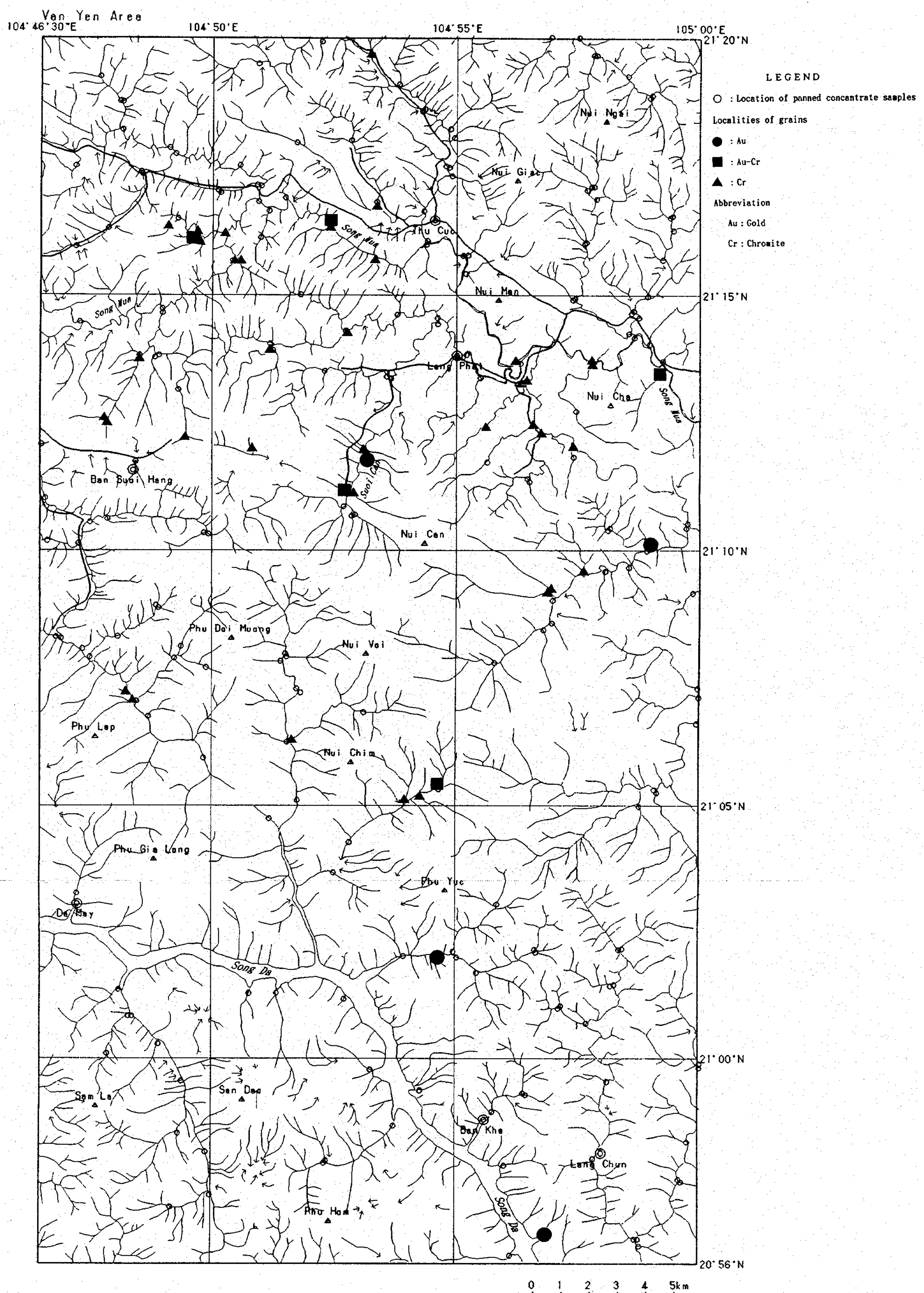


Fig.Ⅲ-2-5 Locality Map of Heavy Minerals in the Van Yen Area

# CHAPTER 3. DETAILED GEOLOGICAL SURVEY OF SUOI BOC - SUOI CU MINERALIZATION ZONE

## 3.1.Geology and Geologic Structure

### 3.1.1. Geology

The geology of the survey area consists of Early Triassic volcanic-pyroclastic rocks and limestone, Middle Triassic sedimentary rocks, and unconsolidated Quaternary sediments in ascending order. Dacite porphyry dikes occur in the area. The dikes are considered to have intruded during Cretaceous time. Figure Ⅲ-3-1 shows the geologic map and geologic sections of this area, and the locality map of soil samples and samples for laboratory studies is given in Plate 10.

The Lower Triassic ($T_1$) occurs in the eastern part of the survey area and is made up of trachybasalt, trachybasaltic tuff, and light grey limestone. The Middle Triassic occupies the major part of the area and is divided into the following two rock facies. That is, one ($T_2s$) comprises clastic rocks which consist chiefly of black mudstone with subordinate amounts of grey to reddish grey fine- to coarse-grained sandstone, grey siltstone, and conglomerate. The sandstone of this rock facies is generally prevalent in the western part of the area, surrounding the Suoi Boc Prospect. The another rock facies ($T_2\ell$) is composed of light grey to dark grey limestone which forms vertical cliffs of 50 m to 100 m high in many places. It seems that the strata of the two rock facies have alternately accumulated. The Quaternary (Q) occurs as a belt in the western lowland extending in the N-S direction. Two small dacite porphyritic bodies ($\tau_6$) are recognized in the vicinity of the northwestern ridge.

### 3.1.2. Geologic structure

The bedding planes are well developed in most mudstone, siltstone, and limestone in the survey area. The beds have generally N-S strikes and steep dips exceeding 50°. Particularly, in the $T_2s$ areas of the south-central and eastern parts, there are steep sequences of nearly vertical beds. It is supposed that the complicated folds have been formed in this area because the area belongs to the "Da River Mobile Belt". From the data obtained through the detailed field survey, it is believed that the major part composed of alternant $T_2s$ and $T_2\ell$ has been folded in a series of N-S trending anticline and syncline with about 500 m wavelength (see Figure Ⅲ-3-1). The Suoi Boc Prospect is situated near the axial plane of the $T_2s$ syncline, and the Suoi Cu mineral showing is on the eastern flank of the $T_2\ell$ syncline.

Four faults of the N-S direction were recognized in the survey area, and NW-SE trending two faults were inferred to occur. The Lower Triassic ($T_1$) is in an N-S trending fault contact with the Middle Triassic ($T_2s$, $T_2\ell$). These N-S trending faults are interpreted to be settled near the axial planes of folds with steep flanks formed by the intense lateral compressional stresses. The vertical displacement by the faults developed within the Middle Triassic area is not known because the stratigraphic relationship between $T_2s$ and $T_2\ell$ is not clear. A fault of the NW-SE direction is inferred to be located on the site of the Suoi Boc Prospect.

### 3.2. Mineralization

The Suoi Boc Prospect and Suoi Cu mineral showing are the representative lead-zinc mineralization zones confirmed by the field survey of the first phase. Prior to the geophysical survey mentioned later in chapter 4, the detailed geological survey was carried out in the whole survey area, but no new mineralization zone similar to the above two has not been discovered. The characteristics of the two mineralization zones are described below.

#### 3.2.1. Suoi Boc Prospect

There are no outcrops but lumps of ore dug out from some pits in this Prospect. Although the tunnel exploration (cross-cut gallery) was carried out by Chinese engineers in this Prospect during 1982 to 1983, the tunnel could not be confirmed at present. In addition to the above, the Mapping Division of GSV dug five pits around the tunnel, but they have collapsed and the details are not clear. According to GSV, the pits were 8 to 10 m deep and mineralization zone of galena and sphalerite was found with 0.1 to 1.0 m width at one pit. One ore sample collected in the survey of Phase I consists mainly of cerussite and sphalerite with a small amount of pyrite, galena, and anglesite. The assay results of the sample are given below. The results show very high contents of lead-zinc.

| Sample No. | Sampling width(m) | Au | Ag | Cu | Pb | Zn | Ni | Cr | Mn |
|---|---|---|---|---|---|---|---|---|---|
| VGM 22 | – | 1 | 431 | 0.025 | 11.9 | 39.4 | 0.002 | 0.009 | 0.053 |

Au is in ppb, Ag in ppm, and other elements in percent.

It has been pointed out through the Phase I survey that this Prospect can be of metasomatic lead-zinc type hosted by limestone. However, on the basis of the results of the detailed survey along the geophysical lines in this phase, this Prospect has a possibility to be of hydrothermal vein type with 2

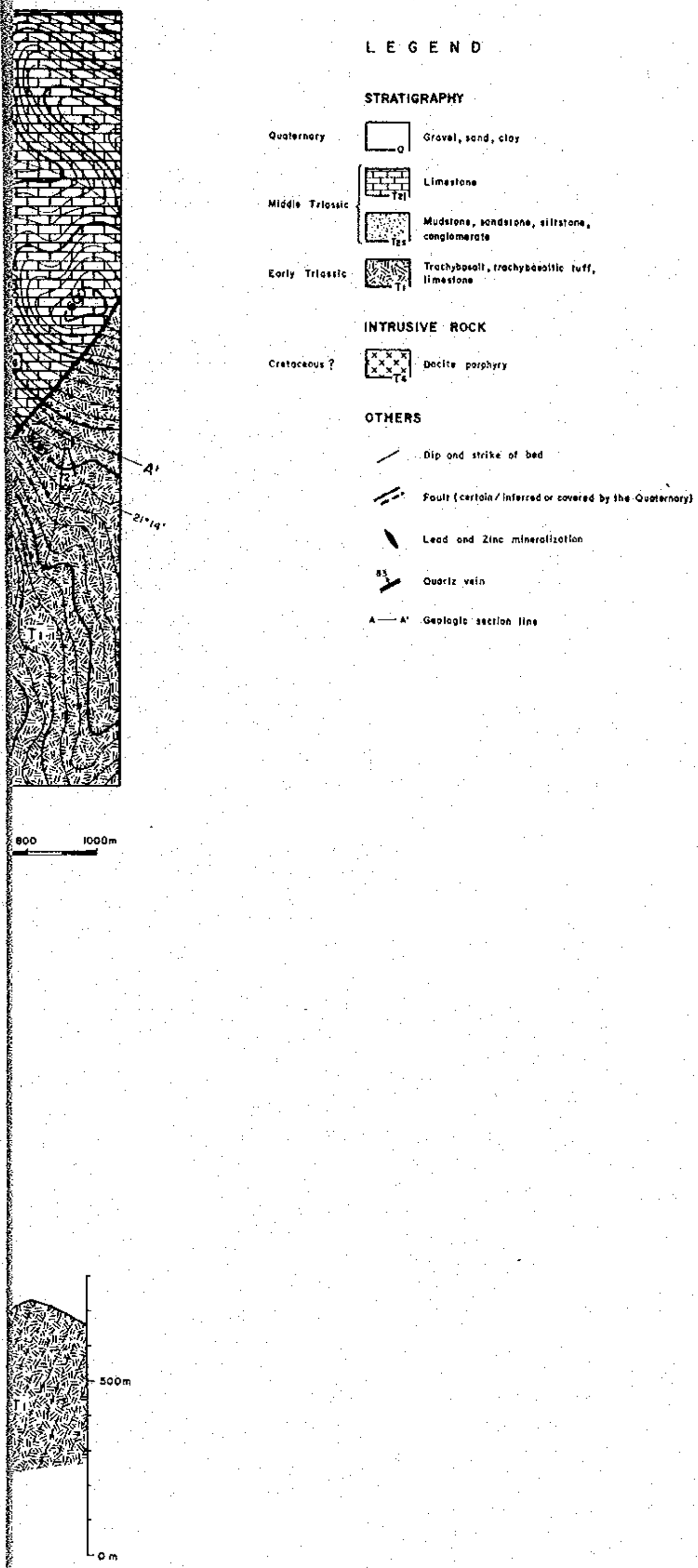


Fig.Ⅲ-3-1 Geologic Map and Sections of the Suoi Boc - Suoi Cu Mineralization Zone

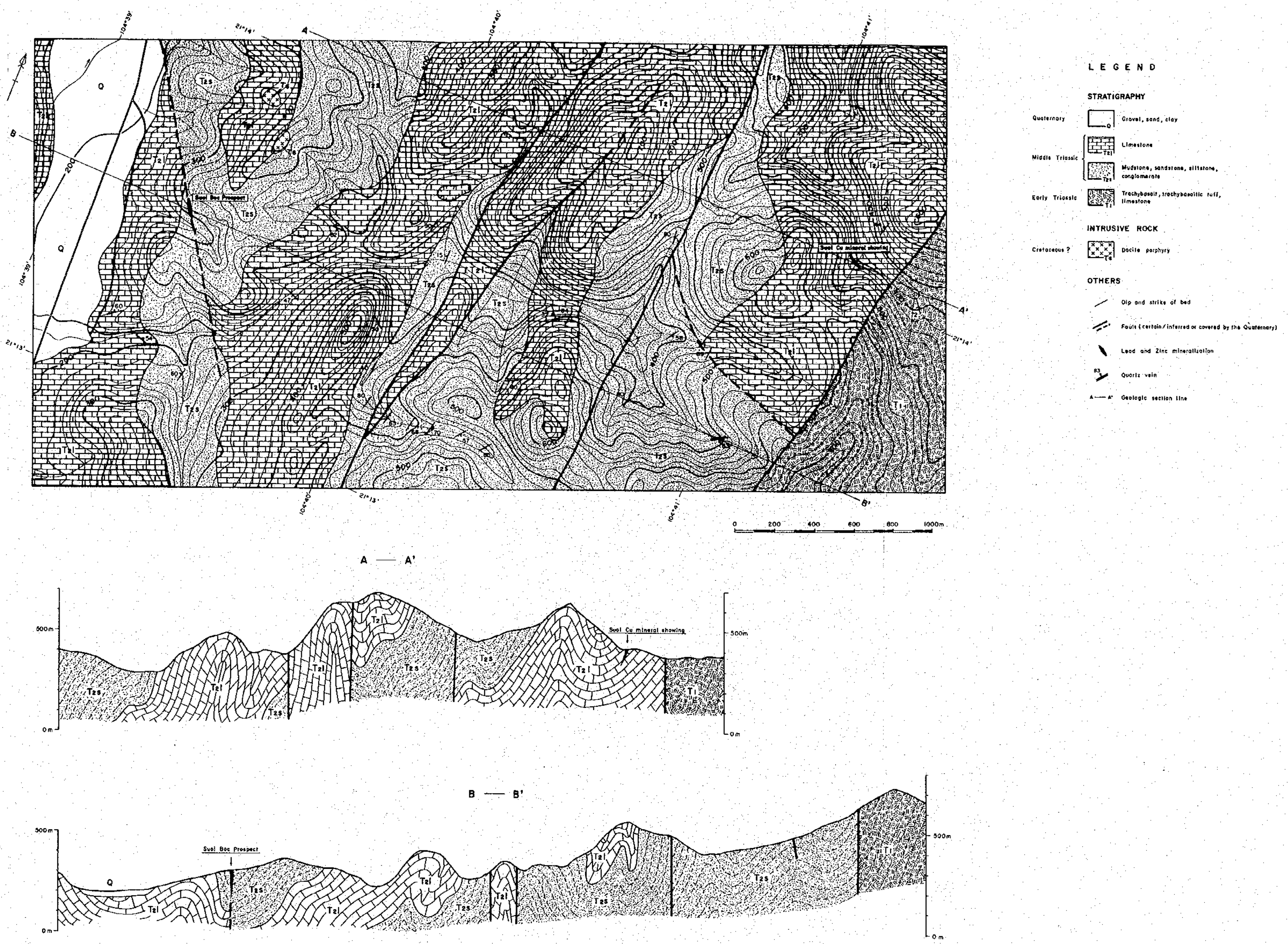


Fig.Ⅲ-3-1 Geologic Map and Sections of the Suoi Boc - Suoi Cu Mineralization Zone

m to 3 m width from the following viewpoints.

1) Five pits are aligned in the direction of N30°W.
2) The Prospect is hosted not by limestone ($T_2\ell$) but by grey fine-grained sandstone ($T_2s$).
3) Some floats of vein quartz were found in and around the stock piles near the pits.

Nevertheless it should be considered that limestone beds can be interbedded in a shallow part from the surface because limestone occurs near the ore body as shown in a geologic section of FigureⅢ-3-1. In this kind of situation, it seems possible that larger deposit than the present ore body would occur hosted by the limestone.

3.2.2. Suoi Cu mineral showing

Trenching was done in two sites by the Mapping Division of GSV in this showing. Dimensions of trenching are 4 to 5 m long, 0.7 to 1.0 m wide, and 1.5 to 3.0 m deep. They are located parallel to the N55°W direction.

One 130 cm x 70 cm massive ore occurs in breccias of limestone at the western wall of the eastern trench, where the matrix consists of soil. The eastern wall of this trench is composed only of breccias of limestone. Thus, the massive ore does not extend eastward.

The massive ore contains mainly smithonite and cerussite with subordinate amounts of sphalerite and anglesite. The limestone is greyish white, fine-grained crystalline, and is recrystallized to marble. Only the breccias of greyish white, fine-grained crystalline limestone were confirmed at the western trench. Ore similar to those of the eastern trench was not found.

The list below shows the assay results of the representative samples collected in the survey of PhaseⅠ.

| Sample No. | Sampling width(m) | Au | Ag | Cu | Pb | Zn | Ni | Cr | Mn |
|---|---|---|---|---|---|---|---|---|---|
| VFM 27 | – | 1 | 75 | 0.128 | 25.819 | 28.892 | 0.002 | 0.004 | 0.208 |
| VFM 28 | – | 19 | < 2 | 0.61 | 0.964 | 37.775 | 0.001 | 0.004 | 0.265 |

Au is in ppb, Ag in ppm, and other elements in percent.

This mineral showing is interpreted to be of vein type with the NW-SE direction through the electrical survey conducted by GSV (refer to PartⅡ,